2011

A CLASSIFICATION OF LOWER PALEOZOIC CARBONATE-BEARING ROCKS FOR GEOTECHNICAL APPLICATIONS

Bethany L. Overfield
University of Kentucky, boverfield@uky.edu

ABSTRACT OF THESIS

A CLASSIFICATION OF LOWER PALEOZOIC CARBONATE-BEARING ROCKS FOR GEOTECHNICAL APPLICATIONS

An empirically-based classification of lower Paleozoic carbonate-bearing rocks was created for field-based geotechnical applications. Geotechnical parameters were subsequently correlated to that classification. Seven hundred seventy-seven samples were used as the basis for the classification. Thirteen categories based on visual and tactile properties and a hydrochloric acid test were created. Samples were from central, north-central, and south-central Kentucky and represented the majority of Ordovician exposures in the state, and some Mississippian exposures. Few Silurian and Devonian units were included in the sample set. Geotechnical parameters, including density as well as elastic constants (shear and compression wave velocities, Poisson's ratio, Young's modulus, and shear modulus), were calculated for 113 representative samples from the classification. Compression strength testing was completed on 29 samples and the slake durability index was calculated for 18 samples. Testing values were correlated to the classification system in an attempt to use the classification as a predictive and comparative tool for geotechnical applications. Despite samples being heterogeneous and isotropic, each of the 13 categories behaved differently and predictably, with the sharpest contrast in siliciclastic and carbonate rocks.

KEYWORDS: cored rocks, sonic velocity, elastic parameters, geotechnical, classification

Bethany L. Overfield

May 2011

CLASSIFICATION OF LOWER PALEOZOIC CARBONATE-BEARING ROCKS FOR GEOTECHNICAL APPLICATIONS

By

Bethany L. Overfield

Gerald A. Weisenfluh

Co-Director of Thesis

Edward W. Woolery

Co-Director of Thesis

Alan E. Fryar

Director of Graduate Studies

May 2011

RULES FOR THE USE OF THESES

Unpublished theses submitted for the Master's degree and deposited in the University of Kentucky Library are as a rule open for inspection, but are to be used only with due regard to the rights of the authors. Bibliographical references may be noted, but quotations or summaries of parts may be published only with the permission of the author, and with the usual scholarly acknowledgments.

Extensive copying or publication of the thesis in whole or in part also requires the consent of the Dean of the Graduate School of the University of Kentucky.

A library that borrows this thesis for use by its patrons is expected to secure the signature of each user.

Name Date

THESIS

Bethany L. Overfield

The Graduate School

University of Kentucky

2011

A CLASSIFICATION OF LOWER PALEOZOIC CARBONATE-BEARING ROCKS FOR GEOTECHNICAL APPLICATIONS

THESIS

A Thesis submitted in partial fulfillment of the
requirements for the degree of Master of Science in the
College of Arts and Sciences
at the University of Kentucky

By

Bethany L. Overfield

Lexington, Kentucky

Co-Directors: Dr. Gerald A. Weisenfluh, Adjunct Professor of Geological Sciences
and Dr. Edward W. Woolery, Professor of Geological Sciences

Lexington, Kentucky

2011

Table of Contents

Table of Contents iv

List of Tables vi

List of Figures vii

CHAPTER 1: INTRODUCTION 1

Problem, Background, and Objectives 1

Location and Geologic Setting 4

Generalized Stratigraphy 6

CHAPTER 2: METHODOLOGY 10

Core Selection 10

Sampling 10

Lithologic Classification 11

Test Sample Selection and Preparation 12

Sonic Velocity Testing 14

Elastic Constants 16

Unconfined Compressive Strength Testing 16

Slake Durability 18

CHAPTER 3: RESULTS AND DISCUSSION 20

Core Selection and Sampling 20

Classification 23

Sample Set 31

Rock Density 32

Density Discussion 33

Sonic Velocity of Samples 34

Compression Waves 34

Shear Waves 35

Velocity Discussion 36
Effect of Density on Velocity Discussion 38
Other Elastic Constants 41
Poisson's Ratio 41
Shear Modulus 43
Young's Modulus 44
Elastic Constants Discussion 45
Unconfined Compressive Strength 47
Unconfined Compressive Strength Discussion 48
Unconfined Compressive Strength versus Velocity Discussion 49
Unconfined Compressive Strength versus Young's Modulus Discussion 50
Slake Durability 51
Slake Durability Discussion 52
CHAPTER 4: CONCLUSIONS 53
Sampling and Classification 53
Density and Velocity 54
Elastic Constants 54
Index Properties 55
General Conclusions 55
APPENDIX 57
REFERENCES CITED 70
Vita 72

List of Tables

TABLE 3.1. ABBREVIATED CLASSIFICATION TABLE. 31
TABLE 3.2. DENSITY OF COMMON ROCKS TYPES (BURGER, 1992). 34
TABLE 3.3. ELASTIC COEFFICIENTS AND VELOCITIES FOR SELECTED COMMON ROCKS. ADAPTED FROM BURGER (1992). 37
TABLE 3.4. AVERAGE ELASTIC COEFFICIENTS AND VELOCITIES FOR EACH LITHOLOGIC GROUP IN THE STUDY SAMPLE SET.....38
TABLE 3.5. DENSITY AND SHEAR WAVE VELOCITY TREND ANALYSES. 40
TABLE 3.6. DENSITY AND COMPRESSION WAVE VELOCITY TREND ANALYSES.....41
TABLE 3.7. COMMON VALUES FOR POISSON'S RATIO (GERCEK, 2007). 46
TABLE. 3.8. YOUNG'S MODULUS VALUES. MODIFIED FROM WEST (1994).....47
TABLE 3.9. COMPRESSIVE STRENGTH BY LITHOLOGY (WEST, 1994).....49

List of Figures

FIGURE 1.1. CARBONATE-BEARING ROCKS IN KENTUCKY. 5
FIGURE 1.2. BASIC GEOLOGIC MAP WITH OUTLINED STUDY AREA. 6
FIGURE 1.3. ORDOVICIAN, MISSISSIPPIAN, AND SILURIAN/DEVONIAN STRATIGRAPHIC COLUMNS. 9
FIGURE 2.1. AN EXAMPLE ARRAY SHOWING PERCENTAGE OF SHALE. 12
FIGURE 2.2. MACHINERY USED FOR SAMPLE PREPARATION TO MEET ASTM PARALLELISM STANDARDS. ROCK SAW (LEFT), DISC SANDER (RIGHT). 13
FIGURE 2.3. MEASURING CORE SAMPLE LENGTH (BY QUADRANT) TO CHECK FOR PARALLELISM CRITERIA. 13
FIGURE 2.4. COMPRESSION AND SHEAR WAVEFORM EXAMPLES. 15
FIGURE 2.5. UNCONFINED COMPRESSIVE STRENGTH TESTING MACHINE AT THE KENTUCKY TRANSPORTATION CABINET. 17
FIGURE 2.6. COMPRESSIVE STRENGTH SAMPLES. 17
FIGURE 3.1. CORE LOCATION MAP. 20
FIGURE 3.2. STRATIGRAPHY OF ORDOVICIAN AND SILURIAN UNITS. BLUE BOLDED, ITALICIZED UNITS WERE SAMPLED. 21
FIGURE 3.3. STRATIGRAPHY OF DEVONIAN AND MISSISSIPPIAN UNITS. BLUE BOLDED, ITALICIZED UNITS WERE SAMPLED. 23
FIGURE 3.4. FINE-GRAINED HOMOGENEOUS LIMESTONE SAMPLES. MASSIVE (56-6) AND MOSAIC/STYOLITE (83-2S) FABRIC REPRESENTATIONS. 25
FIGURE 3.5. COARSE-GRAINED HOMOGENEOUS LIMESTONE. FOSSIL FRAGMENT GRAINS (25-7), PREDOMINANTLY CALCIUM CARBONATE COMPOSITION (78-1S), LAYERED (85-8S), DARK (68-3S), AND LIGHT (78-1S) REPRESENTATIONS. 25
FIGURE 3.6. HETEROGENEOUS LIMESTONE. NODULAR (1-7), STREAKED (32-6 +S), COARSE-GRAINED (51-4), AND FINE-GRAINED (49-1) REPRESENTATIONS. 26
FIGURE 3.7. HETEROGENEOUS LIMESTONE. BIOTURBATED (47-2S), VUGGY (65-3S), SHALY LIMESTONE (40-5), AND LAYERED (84-3S) REPRESENTATIONS. 27
FIGURE 3.8. SHALE. BLACK (74-4S), MASSIVE DARK GRAY (14-5), GRAIN-ORIENTED DARK GRAY (5-6), AND SANDY SHALE (62-5S) REPRESENTATIONS. 28
FIGURE 3.9. FISSILE SHALE. 28
FIGURE 3.10. SILTSTONE AND SANDSTONE. SANDY/STREAKED LAYERED SILTSTONE (69-6S) (62-2S), BIOTURBATED SILTSTONE (71-2S) REPRESENTATIONS, ALONG WITH SANDSTONE (52-SPT-1). 29
FIGURE 3.11. INTERBEDDED LIMESTONE AND SHALE. FOSSIL-FRAGMENT DOMINATED (26-5S), LIMESTONE-DOMINATED (16-19), AND BOTH FOSSIL FRAGMENT AND LIMESTONE (27+1+S) REPRESENTATIONS. 29

FIGURE 3.12. CLASSIFICATION FLOW CHART. 30
FIGURE 3.13. POPULATION DISTRIBUTION OF PREPARED SAMPLE LITHOLOGIES. 32
FIGURE 3.14. DENSITY VALUES DISPLAYED BY LITHOLOGY. 33
FIGURE 3.15. COMPRESSION-WAVE VELOCITY VALUES DISPLAYED BY LITHOLOGY. 35
FIGURE 3.16. SHEAR WAVE VELOCITY VALUES DISPLAYED BY LITHOLOGY. 36
FIGURE 3.17. COMPRESSION WAVE VELOCITY VERSUS DENSITY. 39
FIGURE 3.18. POISSON'S RATIO RESULTS DISPLAYED BY LITHOLOGY. 42
FIGURE 3.19. POISSON'S RATIO VERSUS LITHOLOGY (WITH OUTLIERS REMOVED). 43
FIGURE 3.20. SHEAR MODULUS VERSUS LITHOLOGY. 44
FIGURE 3.21. YOUNG'S MODULUS RESULTS DISPLAYED BY LITHOLOGY. 45
FIGURE 3.22. UNCONFINED COMPRESSIVE STRENGTH VALUES DISPLAYED BY LITHOLOGY. 48
FIGURE 3.23. SHEAR WAVE VELOCITY VERSUS UNCONFINED COMPRESSIVE STRENGTH. 50
FIGURE 3.24. YOUNG'S MODULUS VERSUS UNCONFINED COMPRESSIVE STRENGTH. 51
FIGURE 3.25. SLAKE DURABILITY INDEX VERSUS LITHOLOGY. 52

CHAPTER 1: INTRODUCTION

Problem, Background, and Objectives

Geotechnical engineers and geologists describe and measure the physical properties of rocks to determine their expected behavior. Physical properties are assessed at two distinct scales: on small-scale samples in the laboratory and on large-scale masses of rock in the field. Field-based studies on in situ larger-scale rock volumes or "rock mass" properties are constrained or controlled both by the individual rock types and discontinuities that bound and intersect them. "Intact rocks" are not used to assess discontinuities, but to measure rock matrix properties in smaller laboratory samples (West, 1994). Intact rock strength partially governs rock mass strength (Hack and Huisman, 2002) and provides the scale for this study.

As an example, the Kentucky Transportation Cabinet conducts between 200 and 300 geotechnical rock studies for transportation structure designs every year. As many as 50 coreholes are drilled for each project to obtain samples for both sedimentary rock and soil evaluations. Before the cores are sampled and tested, they are first described by geologists or geotechnical engineers. The descriptions assess rock elements that relate to strength and durability, such as gross lithology, weathering, fracturing, and physical integrity. Lithologic descriptions generally do not include types of sedimentary structures or rock fabrics that relate to sedimentary origin. A number of tests or evaluations are performed on the rock specimens based on the uses of the materials for the project. Specifically, quantitative and semiquantitative lab tests are conducted on rock samples, including slake durability index, jar slake, and unconfined compressive strength. Slake durability testing is performed on argillaceous rocks (mainly shales) in order to assess resistance to weathering. Argillaceous rocks are susceptible to moisture, which can cause disaggregation, and ultimately lead to foundation, slope, or cut failure. The jar slake test is a relatively quick supplement to the slake durability test that immerses the sample in a beaker of water for a period to evaluate the degree of disaggregation. Unconfined compression strength is one important method for determining rock strength (Farmer, 1983; West, 1994).

Qualitative core evaluations predict in situ rock behavior. This includes measurements of rock quality designation, rock disintegration zone depth, scour potential depth, and allowable bearing capacity. Standard rock quality designation is a core recovery percentage designed to test in situ

rock integrity based on the sum of the pieces of core greater than 4 in. in length divided by the total length of the core. The modified Kentucky rock quality designation method differs in that it estimates rock integrity by counting the number of core pieces at least 4 in. in length that are hard and difficult to break by hand. The rock disintegration zone is the depth to which weathered and decomposed bedrock materials are deemed “rippable” with a D-9 bulldozer. Scour potential is assessed for those rocks that will become the foundation of bridge pilings in active streams. As a general rule, shales with a slake durability index of less than 50 percent and a rock quality designation of less than 25 percent are considered potentially scourable. The allowable bearing capacity evaluation is done to assess the capacity of bedrock to bear weight and is assessed only for cores that are located where structures such as bridge pilings will be placed. These standard tests are done in order to evaluate engineering characteristics. Rock evaluations are based in part on visual inspection of core. A goal in this study was therefore to include more descriptive properties, such as mineral grain composition, bedding, and texture, to improve the understanding of relationships between rock units and their field performance.

To assess rock properties and engineering characteristics, a more systematic approach for sample comparison was first needed. Although mechanical rock testing is the most accepted and dependable way to measure rock properties, the resultant characteristics cannot be effectively extrapolated more broadly without identifiable correlative visual indices. This requires a system of rock description that is both comprehensive and repeatable.

Primary rock properties affecting rock strength and durability are mineral grain composition, cementation, grain size (texture), bedding, crystallinity, and fabric; however, coherency of these properties is rarely communicated in core descriptions. Geotechnical rock descriptions are often recorded as text paragraphs with parenthetical comments. Specifically, lithologic descriptions are rooted in major categories of composition and texture with additional comments pertaining to properties that the observer thought were important. For example, “gray shale with limestone layers” was the extent of one description, whereas another description was “limestone: gray, fine to med, crystalline, argillaceous, w/ shale partings, even to nodular bedding, fossiliferous.” Consequently, descriptions vary considerably and lack a uniform format. Hence, uniformity among descriptions is very difficult to discern. A standard descriptive system or method specifically tailored for geotechnical applications would help geologists and geotechnical engineers accurately and uniformly describe core.

Current classifications, such as that of Deere and Miller (1966), use unconfined compressive-strength intact-rock classification, without regard to rock lithology. Some classifications are theoretically based, such as ternary diagrams that are subdivided based on end-member mineral compositions. Theoretical classifications have two shortcomings—not all positions in the diagram occur in nature, and they only use a limited number of properties for categorization. Empirical classifications are based on a finite set of samples, but are likely to encompass the domain of interest. Examples of empirically based classification systems created for coal-bearing sedimentary rocks are those of Ferm and Smith (1981), Ferm and Weisenfluh (1981), Ferm et al. (1985), and Barnhill and Zhou (1996). These pictorial core manuals are used by drillers, engineers, and geologists for logging coal cores; they are quick and simple to use but retain the maximum amount of information possible. Manuals resulted in a classification that encompassed important properties (mineral composition, grain size, color, and sedimentary structures) of the subject rocks into a single term and an intuitive numeric system for rendering the different rock types in computer systems. Because these methods had a high level of repeatability, they were useful for comparative analysis.

If standard descriptions are utilized, core parameters can be correlated with useful technical design parameters. For example, Molina and Mark (1996) applied the Ferm classification system to the characterization of coal mine roof rock by correlating strength parameters to classified core samples. This was done primarily for coal mine hazard assessment, mine reinforcement, and mine entry design. Relative roof strength was ranked based on axial and bedding plane strength and ratings were assigned to the common lithologies found in the core manual. Smath (1983) used the Ferm classification system in an effort to correlate lithology and engineering parameters such as point load testing and slake durability.

The Ferm and Weisenfluh (1981) classification covers Pennsylvanian rocks in Kentucky; however, two-thirds of the state is underlain by lower Paleozoic carbonate-dominated rocks. Considering that the majority of siliciclastics in the state have been classified as Pennsylvanian, there was an interest in creating a similar classification for carbonate-bearing rocks. Classification schemes concentrating on carbonate-bearing rocks have been developed by Folk (1959) and Dunham (1962), and both are widely used by geologists. Dunham's classification is based on texture and is used more readily in the field, whereas the Folk classification is based on carbonate components and matrix and is more useful in the laboratory with the aid of microscopy. Both

methods were developed for assessing depositional setting and require some geologic training in the description of carbonate (chemical) grains and cements. Neither classification addresses the interbedding of limestone, dolomite, and siliciclastic lithologies that is prevalent in Kentucky. Consequently, an empirical classification for Ordovician to Mississippian carbonates was the first objective of this thesis. Specifically, this study constructed an empirical, repeatable classification of carbonate-bearing rock in Kentucky that can be compared between sites, and assesses observed properties (such as lithology, grain size, bedding, and fabric) that relate to rock behavior. Many of the current standard-of-practice tests are inefficient to conduct; therefore devising a quick and inexpensive proxy test method that can approximately predict properties such as strength and durability is a goal.

Sonic velocity measurements are an example of a proxy test that assesses elastic rock properties. Sonic velocity measurements on core specimens are influenced by many of the properties that affect rock behavior (lithology, grain size, bedding, etc.) and the test is relatively efficient and nondestructive. A number of studies focusing on the correlation between physical properties of cored rocks (i.e., lithology) and engineering parameters (i.e., rock strength and wave velocities) have been conducted (Johnston and Christensen, 1993; Jones and Wang, 1981; King, 1998); however, little has been done to explore the applications of the correlation between rock properties and engineering parameters for transportation construction. The second objective of this thesis was, therefore, to ascertain if sonic velocity can be effectively used as a predictive and comparative tool for elastic rock properties and whether it can be related to lithologic descriptions.

Location and Geologic Setting

Kentucky is an ideal place to develop a classification of carbonate and associated rocks because of the wide variety of Paleozoic carbonate-bearing units exposed at or near the surface in the state. More than 35 percent of the state is underlain by carbonate-bearing formations (Figure 1.1).

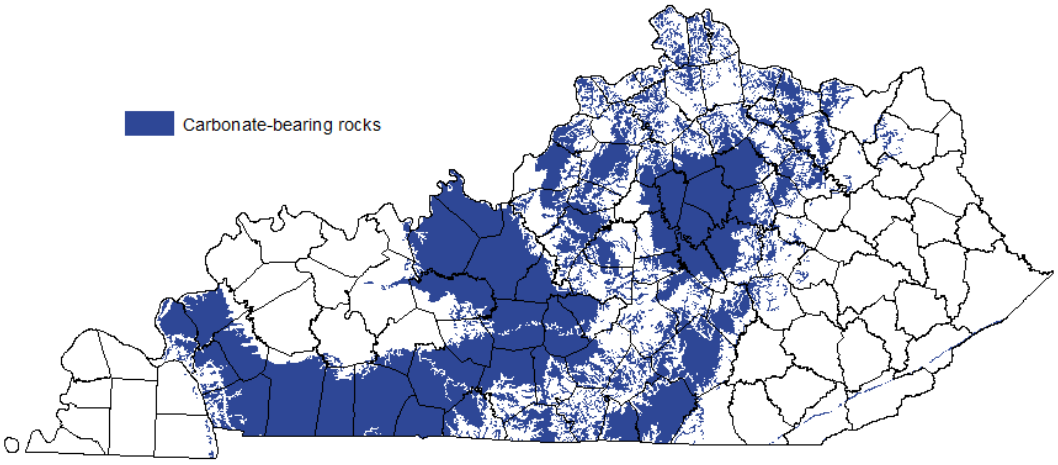

Figure 1.1. Carbonate-bearing rocks in Kentucky.

Ordovician rocks found at or near the surface in central and north-central Kentucky (Figure 1.2) contain a variety of different carbonates with varying geotechnical properties; therefore, this area was chosen to begin the carbonate classification process. Areas adjacent to the initial study area that include Mississippian rocks, and to a lesser degree, Silurian and Devonian rocks, also have good carbonate-bearing exposures, and some of these areas were eventually included in the study.

Kentucky Transportation Cabinet cores were requested by and used for this study based on the cabinet's districts. As a result, cabinet districts make up the study area boundary. Districts 5, 6, and 7 encompass all of north-central, central, and south-central Kentucky and include all of the Ordovician carbonate-bearing rocks of interest (as well as some Silurian and Devonian units) and therefore were used to select recent geotechnical projects with candidate cores (Figure 1.2). Many of the largest population centers in the state are situated in the study area; thus, more roadway construction projects are found here. The extent of the study area was designed to maximize core availability and bedrock type. To expand the classification to include some Mississippian carbonate-bearing rocks, a part of Transportation Cabinet District 8 was also sampled, and the study area boundary therefore includes south-central Kentucky.

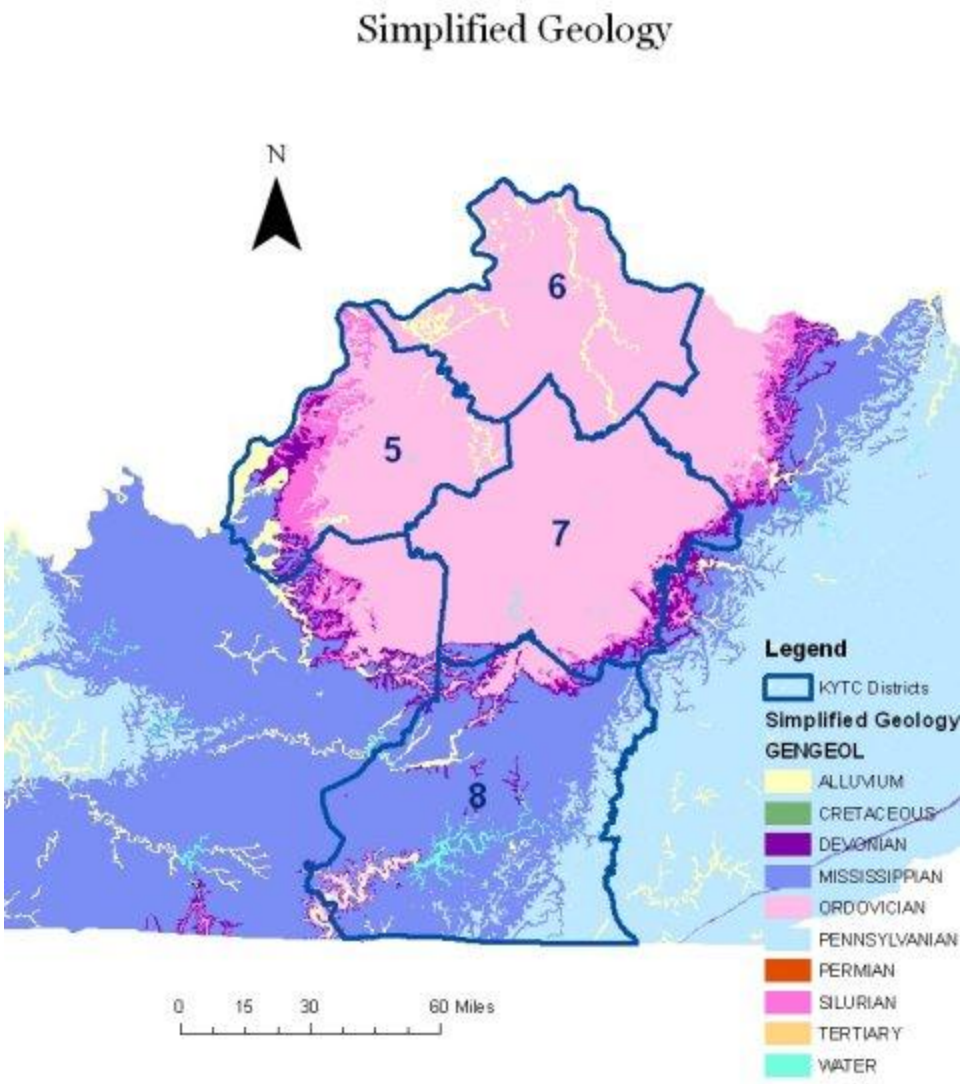

Figure 1.2. Basic geologic map with outlined study area.

Generalized Stratigraphy

Approximately 1,400 ft of the Ordovician System—the oldest exposed system in the state—is preserved in central Kentucky (Figure 1.3). The base of the exposed Ordovician is the Middle Ordovician High Bridge Group, which comprises the Camp Nelson Limestone, Oregon Formation, and Tyrone Limestone, in ascending order. This group, at its thickest, is 440 ft (McDowell, 1986). The High Bridge Group is overlain by the Middle Ordovician Lexington Limestone, which is 320 ft at its thickest. The Lexington Limestone is composed of a complex mosaic of mapped members.

In ascending order, they are the Curdsville Limestone Member (20−40 ft thick), Logana Member (up to 50 ft thick), Grier Limestone Member (100−180 ft thick), Brannon Member (up to 30 ft thick), Tanglewood Limestone Member (occurring in multiple layers), Sulphur Well Member (up to 35 ft thick), Millersburg Member (90 ft thick), Stamping Ground Member (15 ft thick), Devil's Hollow Member (up to 30 ft thick), and Strodes Creek Member (Cressman, 1973). The Lexington Limestone is overlain by several Upper Ordovician units, many of which are laterally correlative, beginning with the Clays Ferry Formation (90−300 ft thick), Kope Formation (200−275 ft thick), and Garrard Siltstone (up to 100 ft thick), which make up the lower part. The Calloway Creek Limestone (60−150 ft thick) and correlative Fairview Formation (40−130 ft thick) are next, followed by the Grant Lake Limestone (3−160 ft thick) and correlative Ashlock Formation (up to 80 ft thick). These units are overlain by the Bull Fork Formation (90−240 ft thick) and the Drakes Formation (20−150 ft thick) (Weir et al., 1984).

Silurian rocks are situated above Ordovician rocks (Figure 1.3). The basal contact of the Silurian is an erosional unconformity in some areas and conformable and paraconformable in other areas. The Silurian System ranges in thickness from 0 to 300 ft and stratigraphically ascends in the following order: Brassfield Dolomite (10−30 ft thick), Osgood Formation (10−50 ft thick), Laurel Dolomite (40−65 ft thick), Waldron Shale (9−15 ft thick), and Louisville Limestone (up to 95 ft thick) (McDowell, 1986).

The Devonian System in Kentucky rests unconformably on both Silurian and Ordovician units (Figure 1.3). A carbonate sequence, the Jeffersonville Limestone and Sellersburg Limestone of the Middle Devonian (up to 50 ft thick), makes up the base in the study area. These units are overlain by the Upper Devonian New Albany Shale (up to 110 ft thick) (McDowell, 1986).

The Mississippian System varies considerably stratigraphically because of its wide distribution throughout the state resulting in regional differences in depositional setting. In the scope of this study area, the units, from oldest to youngest are the Early Mississippian Borden Formation, comprising the New Providence Shale Member (120−250 ft thick), Kenwood Siltstone Member, Nancy Member (150−300 ft thick), Holtsclaw Siltstone Member/Halls Gap Member (both generally less than 100 ft, but at times up to 250 ft thick), Floyds Knob Bed/Wildie Member, and Muldraugh Member/Fort Payne Formation (up to 660 ft thick). The Upper Mississippian begins with the Salem Limestone/Salem and Warsaw Formations at the base and is overlain by the St. Louis Limestone (70−160 ft thick), Ste. Genevieve Limestone Member (30−90 ft thick), and

Kidder Limestone (90−230 ft thick), in ascending order (McDowell, 1986; Sable and Dever, 1990). It was not possible to sample all units of the Mississippian in Kentucky; therefore, not all lithologies are represented in this study.

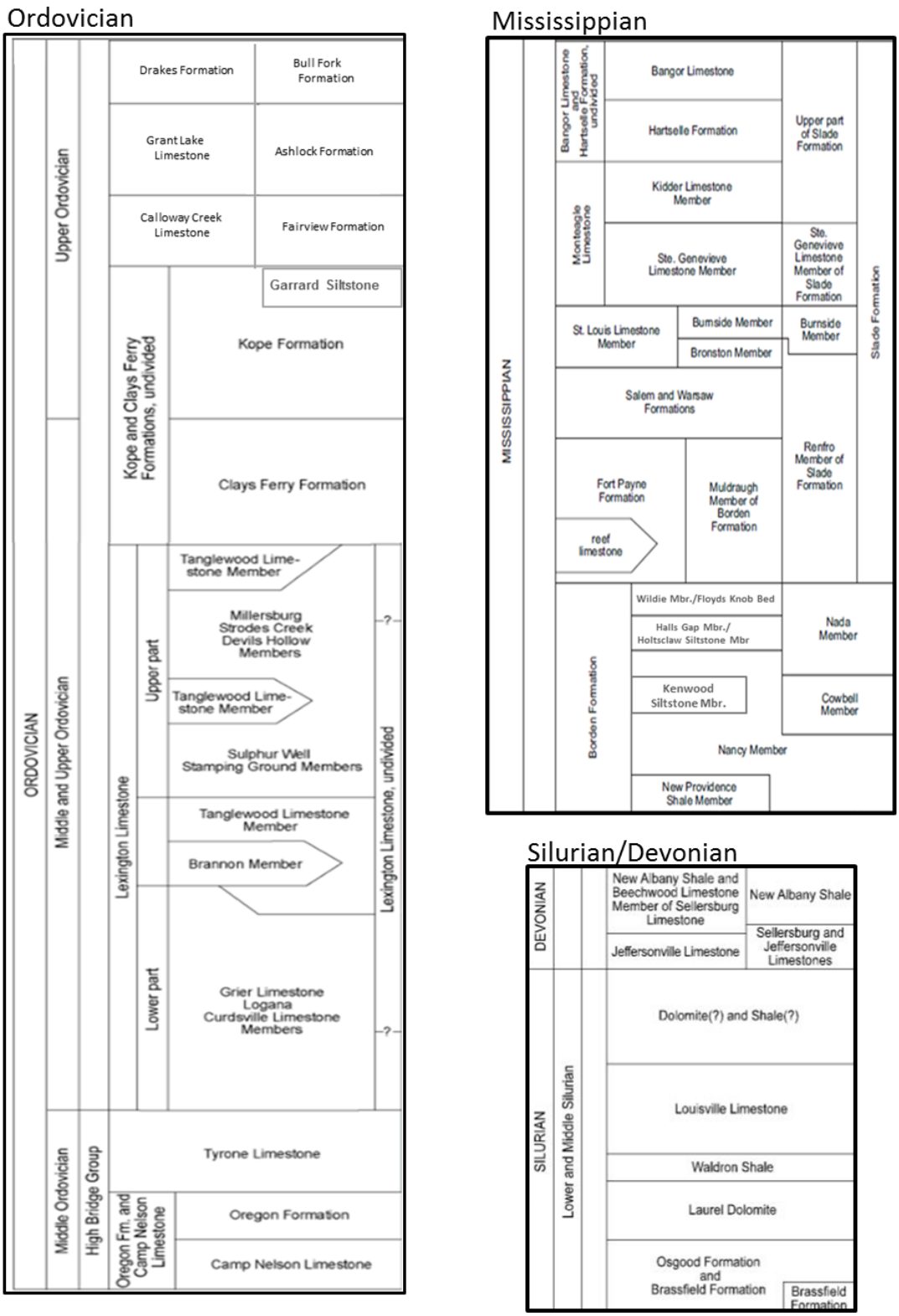

Figure 1.3. Ordovician, Mississippian, and Silurian/Devonian stratigraphic columns.

CHAPTER 2: METHODOLOGY

Core Selection

Recently drilled Kentucky Transportation Cabinet cores (generally within the past 10 years) were selected based on stratigraphic position in the study area. Cores were requested from the cabinet based on approximate stratigraphic position, but the exact stratigraphic range of each core was not certain because of generalized core locations (locations were most often not given in a coordinate system) and the possibility of subsurface contacts at depth (subsurface holes often penetrate formation boundaries). An attempt was made to acquire cores from each county of the study area, representing all bedrock geologic units of the Upper and Middle Ordovician, Lower Silurian, and Mississippian. An additional deep core (1,002 ft) from Clark County (from a Kentucky Geological Survey project) was used for sampling. Only the most recent projects include surveyed geographic coordinates for the holes; therefore, most hole locations were estimated by comparing design drawings to georeferenced map images showing the built infrastructure.

Sampling

Cores were sampled in order to create a reference collection of all lithologies in the study area for targeted stratigraphic units. Although stratigraphic identification of sampled units was not a priority, efforts were made to obtain cores from the greatest spread of stratigraphic units. Samples were selected from each core based on observed lithologic differences. Samples 3 to 8 in. in length (the necessary length for subsequent testing parameters) were taken from each recognizable rock layer, even if that lithology occurred repeatedly. This method produced the most representative sampling, as it reflected the frequency of occurrence of the different kinds of rock. Boundaries between lithologies were determined and a random sample was collected from each delineated unit. The sampling technique for the Clark County core differed because of the core depth, which was more than 1,000 ft. For this core, one sample was taken out of each box of core. Each box contained approximately 20 to 25 ft of core; thus, 113 samples were taken from that location. After all cores were sampled, the sample set approximated the frequency of occurrence (although not the volumetric occurrence) of rock types in the study area.

Sample depth was recorded for each specimen, and sample orientation (top) was marked. All samples were given a unique identification number. Although cores were requested based on stratigraphic range, specimens were not labeled with respect to geologic units to avoid bias during the classification procedure.

Lithologic Classification

A standard descriptive system focusing on field-based assessments was created to enable geologists and geotechnical engineers to uniformly describe core. Because sample identification would take place in the field, it was necessary for the methodology to be based on visual and tactile properties and simples tests (such as hydrochloric acid). Sample specimens were initially grouped based on observations of gross lithology. Siliciclastic rock samples were separated from carbonate rock samples to get a preliminary idea of the types and frequency of occurrence of rocks that were sampled. General lithologic groupings included sandstone, siltstone, shale, limestone, dolostone, and interbedded limestone and shale (at the scale of a 3- to 8-in. core sample). In order to differentiate carbonate-bearing rocks from siliciclastic rocks, simple hydrochloric acid tests were used for observable carbonate effervescence.

After this initial categorization, megascopic rock properties were used to further refine the classification. These properties were (1) lithology, (2) percentage of carbonate components, (3) apparent (visual) mineral composition, (4) grain size, (5) bedding structure, (6) fabric, and (7) color. Sample “arrays” were used to identify the variability of each property of interest within the sample set. All relevant samples were arranged on a table in order of the variation of each single property (e.g., percentage of shale). Samples with similar properties were placed at the same horizontal position along an array above previously positioned pieces. The resulting displays (Figure 2.1) often looked like a standard histogram. They showed the total range in variation of the property, identified natural groupings, and accounted for the frequency of occurrence of each subtype. Property class boundaries were defined along the array with the objective of minimizing the total number of classes (too many classes lead to poor repeatability) and placing the boundaries at positions where the sample frequency was low. This method was thought to be the closest representation of natural groupings and leads to a more repeatable method. The resulting classification was informally tested for repeatability by asking other geologists to assign test specimens to a group based on specified criteria. Boundaries that were

found to be easily recognizable and consistently identified by practitioners were retained for the final classification.

With the diversity of the samples in mind, a flow chart was created that would be used as a guide to classify each sample. The creation of the flow chart was an iterative process, the goal of which was to lead the practitioner to classify core samples based on the classification that had been defined by the arrays.

Figure 2.1. An example array showing percentage of shale.

Test Sample Selection and Preparation

One hundred fifteen representative samples were selected for further testing based on lithology, sample length, and sample integrity (unbroken samples). Selected samples representing all lithologic units were at least 2 in. long, and were one continuous piece without fractures or other discontinuities. They were prepared for ultrasonic velocity testing in accordance with ASTM standard D 2845-05 (ASTM, 1984). For this test, a parallelism requirement had to be met, which dictated that sample core ends had to be parallel within

0.005 in. To achieve this, core ends were sawed using a diamond wet saw and sawed surfaces were then sanded flat with a circular disc sander (Figure 2.2).

Figure 2.2. Machinery used for sample preparation to meet ASTM parallelism standards. Rock saw (left), disc sander (right).

Some interbedded samples and shale samples were only sanded and not sawed, because of issues with fragility when the samples were exposed to moisture. In order to test for parallelism, core ends were divided into quadrants and crosshairs were aligned and drawn on each end. Calipers were used to take measurements at four labeled points (Figure 2.3).

Figure 2.3. Measuring core sample length (by quadrant) to check for parallelism criteria.

If measurements exceeded the 0.005-in. parallelism standard, the core was sawed or sanded again, or both, and parallelism was once again checked. If parallelism was only slightly off, handheld diamond tool sharpeners (woodworking tool sharpeners) were used to refine the surface.

The length, diameter, and weight of each sample were measured in order to calculate density. The length measurement was based on the average of all quadrant measurements (taken to

check for parallelism) and the diameter measurement was based on the average of measurements taken from the top, middle, and bottom of the core. Length and diameter measurements were taken using a caliper. Density was calculated as follows:

$$\rho = m \div V$$

where:

ρ = density (kg/m^3)

m = mass of sample (kg)

V = volume (m^3)

Meeting parallelism standards frequently proved to be difficult. Although standards were met for every sample, an experiment was conducted on seven samples to evaluate the effect of nonparallelism on sonic velocity results. One end of each sample was sawed at an angle up to 30° to produce nonparallelism. Sonic velocities were measured before and after resawing, and results were compared.

Sonic Velocity Testing

Ultrasonic wave velocities were determined for core samples using the pulse transmission technique first applied by Birch (1960). A system manufactured by the Oyo Corporation of Japan was used and included a high-voltage pulse generator (model-5234) and a new SonicViewer (model-5217A). The pulse generator produces compression and shear waves and is a power booster for the New SonicViewer's transducers. One transducer takes electrical pulses from the generator unit, converts them to ultrasonic mechanical waves, and applies them to the core. The receiving transducer converts the mechanical wave back to electrical form so that arrival times can be measured. The New SonicViewer is an analog device, so graphic representations of the wave arrivals were manually interpreted and then printed for record keeping. Before the two transducers were affixed to each end of a core specimen, a zero adjustment reading was performed in order to account for the several microseconds between the time that the electrical pulse is received and then converted into a seismic pulse. To take a zero adjustment reading, the transducers were placed together and an initial reading was taken (this reading was captured and saved and can be seen above the core sample compression and shear waveforms in Figure

2.4). The first arrival time was used to determine compression wave travel time, and phase differences (trough to trough measurements taking the difference between the zeroed-out trough time and the core sample trough time) were used for shear wave travel times because of the ambiguity of the initial arrival times for shear waves.

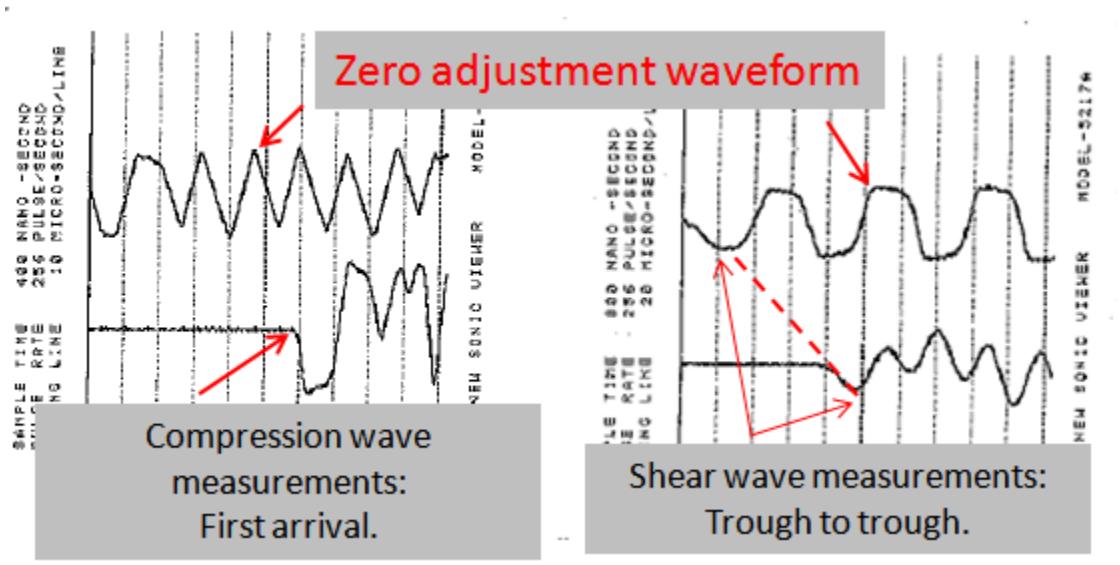

Figure 2.4. Compression and shear waveform examples.

Three transducers using different frequencies were used for compression wave measurements (63 kHz, 200 kHz, and 500 kHz), and two were used for shear wave measurements (33 kHz, 100 kHz). Compression wave velocity was calculated by averaging travel time values from all three transducers; shear wave velocity was calculated using only the 33-kHz transducer values because the majority of the 100-kHz transducer results were inconclusive.

Wave velocity was calculated as follows:

$$V = L \div t$$

V = velocity (m/s)

L = sample length (m)

t = travel time (s).

Elastic Constants

Wave velocities can be used to calculate a number of elastic constants, including Young's modulus, shear modulus, and Poisson's ratio, all of which help define strength parameters of rock. Young's modulus relates the resultant strain to a given stress, and shear modulus is the ratio of shear stress to shear strain. Poisson's ratio is the ratio of transverse contraction strain to longitudinal extension strain in the direction of stretching force (Burger, 1992). The equations are as follows:

$$E = [\rho v_s^2(3v_p^3 - 4v_s^2)]/(v_p^2 - v_s^2)$$

$$G = \rho v_s^2$$

$$\mu = (v_p^2 - 2\,v_s^2)/[2(v_p^2 - v_s^2)]$$

where:

E = Young's modulus (N/m^2)

G = shear modulus (N/m^2)

μ = Poisson's ratio

ρ = density (kg/m^3)

v_s = shear wave velocity (m/s)

v_p = compression wave velocity (m/s).

Unconfined Compressive Strength Testing

The Kentucky Transportation Cabinet performs unconfined compression tests on rocks when designing drill shafts for structures in order to evaluate compressive strength. Testing was performed by the cabinet, mainly on limestone and a few interbedded samples, using Kentucky method 64-523-08, which uses a Tinius Olsen Super L 120K compression tester. Sample preparation standards for unconfined compressive strength testing are quite similar to ultrasonic velocity measurement standards. Sample preparation was therefore already complete. Core samples were placed vertically in a load-bearing apparatus (Figure 2.5) where pressure was applied to both ends of the core along the axial direction. Load was applied until

failure occurred, at which point most samples broke apart. Some samples broke apart explosively into many pieces, whereas the failure of other samples is evident only by a crack (Figure 2.6).

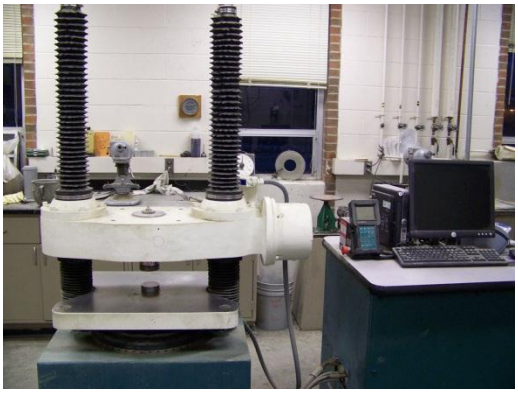

Figure 2.5. Unconfined compressive strength testing machine at the Kentucky Transportation Cabinet.

Figure 2.6. Compressive strength samples.

Unconfined compressive strength was calculated as follows:

$$\alpha_c = F/A$$

where:

α_c= unconfined compressive strength

F = maximum failure load (lb)

A = cross-sectional area of the core (in.^{2}).

Slake Durability

Slake durability testing is used to classify shale and other sedimentary rocks (mainly friable sandstone) to assess resistance to weathering and durability (moisture sensitivity). Testing results are of particular interest in designing rock cut-slope configurations, evaluating scour resistance, and determining the allowable bearing capacity of spread footings for structures. Slake durability testing is conducted if shale is present in a core, and one sample is taken for testing every 5 ft (1.5 m). Since shale deposits in Kentucky are often interbedded with layers of carbonates, distorted slake durability results are common because carbonates do not weather like shales. Slake durability values are often used in conjunction with jar slake results for a more thorough understanding of durability (Table 2.1) (KYTC, 2005). Jar slake values are derived by oven-drying samples and then placing them in beakers, where a numerical designation is given to represent the breakdown of the sample while in the beaker after a specified period using Kentucky method 64-514-08 (KYTC, 2005). To better understand slake durability values for shales in Kentucky, a statewide breakdown of slake durability results collected from 2008 to 2010 is shown in Table 2.1. Thirty-nine percent of samples taken during this time were classified as durable and 61 percent were classified as nondurable.

For the slake durability tests, Kentucky method 64-513-08 was used. Samples were subjected to two standard cycles of drying and wetting. Samples were then broken into approximately 10 pieces weighing 40 to 50 grams each, and placed in a beaker. The beaker and samples were oven-dried for 12 hours at 230° ±9°F. They were weighed in the beaker and then placed in a

2.00-mm standard mesh cylinder in a water-filled test drum, where they were rotated at 20 rpm for 10 minutes. Samples were removed from the drum, oven-dried, and again placed in the water-filled drum. They were then weighed again and the slake durability index was calculated as follows:

$$SDI = (W_2\text{-}B/W_1\text{-}B\ ) * 100$$

where:

SDI = slake durability index (%)

W_1 = weight of the sample after initial drying (g)

W_2 = weight of the sample after the wetting and drying cycle (g)

B = weight of the beaker (g).

Table 2.1. Shale classification based on slake durability index and jar slake values (KYTC, 2005).

Classification	**SDI Range (%)**	**Typical Jar Slake Category**	**2008-2010 Kentucky Transportation Cabinet Statewide SDI Results (1,546 samples)**
Durable	≥ 95	6	39%
Nondurable			
Class I	80 to 94	4 or 5	29%
Class II	50 to 79	3 or 4	21%
Class III	≤ 49	1 or 2	11%

CHAPTER 3: RESULTS AND DISCUSSION

Core Selection and Sampling

A total of 771 samples were obtained from 86 cores in the study area (Figure 3.1). More than 60 percent of the cores were Ordovician, 30 percent were Mississippian, and 6 percent were Silurian and Devonian. The majority of both the Ordovician (Figure 3.2) and Mississippian (Figure 3.3) stratigraphic units cropping out in the study area were sampled.

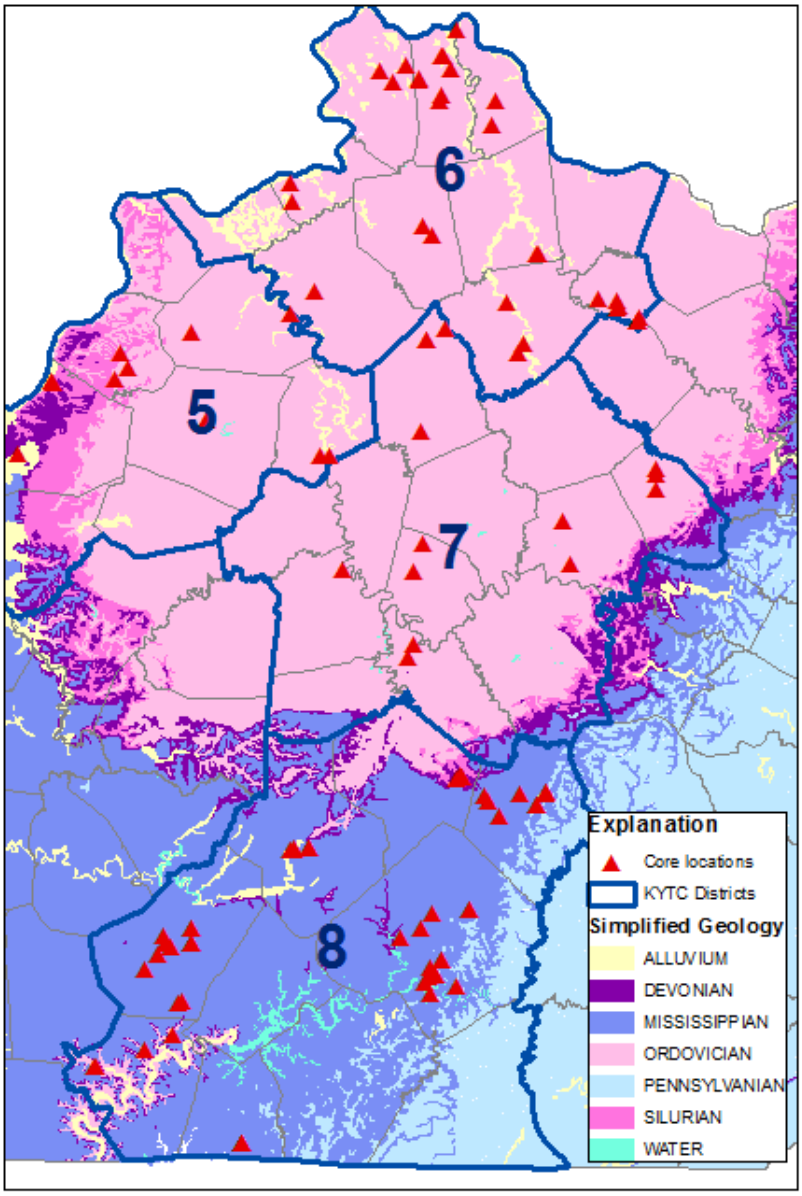

Figure 3.1. Core location map.

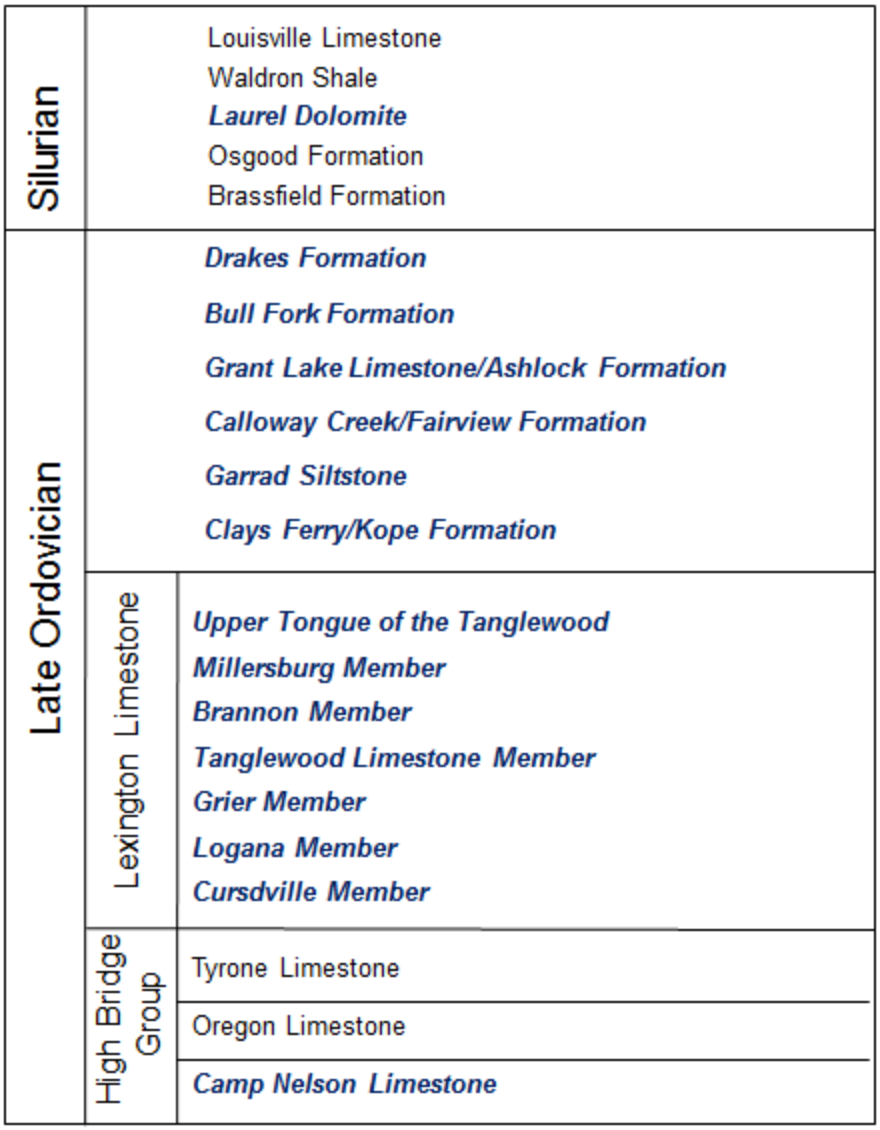

Figure 3.2. Stratigraphy of Ordovician and Silurian units. Blue bolded, italicized units were sampled.

The only formation sampled in the High Bridge Group was the Camp Nelson Limestone, which is micritic with subhorizontal dolomite-filled burrows (Cressman and Noger, 1976). Samples were taken of the Lexington Limestone, which is dominated by very fossiliferous limestone and fossil-fragmental calcarenite (Cressman, 1973). The majority of Ordovician samples came from the Upper Ordovician, which consists of interbedded fossiliferous limestone or dolomite and shale in a variety of units (Weir et al., 1984).

Silurian samples were taken from two units, the Louisville Limestone, a thin-bedded, gray dolomitic limestone and gray calcitic dolomite, and the Laurel Dolomite, a gray dolomite

(Peterson, 1981). Three Devonian cores were sampled: two from the New Albany Shale, which is black, carbonaceous shale, and one from the Sellerbsurg Limestone, a carbonate sequence (McDowell, 1986).

The Lower Mississippian Borden Formation was sampled (Figure 3.3). The lower Borden is made up of terrigenously deposited detrital rocks and is overlain by carbonate-rich beds in the upper part of the unit. The Fort Payne Formation, the uppermost member of the Borden, was sampled. In south-central Kentucky, the Fort Payne consists mainly of dolosiltites that are commonly intensely bioturbated. Upper Mississippian limestone units sampled included the Salem and Warsaw Formations (biocalcarentine, calcareous mudstone, and argillaceous limestone), the St. Louis Limestone (micritic to lutitic carbonate rock with lesser amounts of terrigenous matter in the lower and middle parts of the formation), Ste. Genevieve Formation (oolitic and bioclastic calcarenite, bioclastic calcirudite, gray calcirudite, and finely crystalline dolomite), and the Kidder Limestone (bioclastic and oolitic calcarenite interbedded with calcilutite and dolomite) (Sable and Dever, 1990).

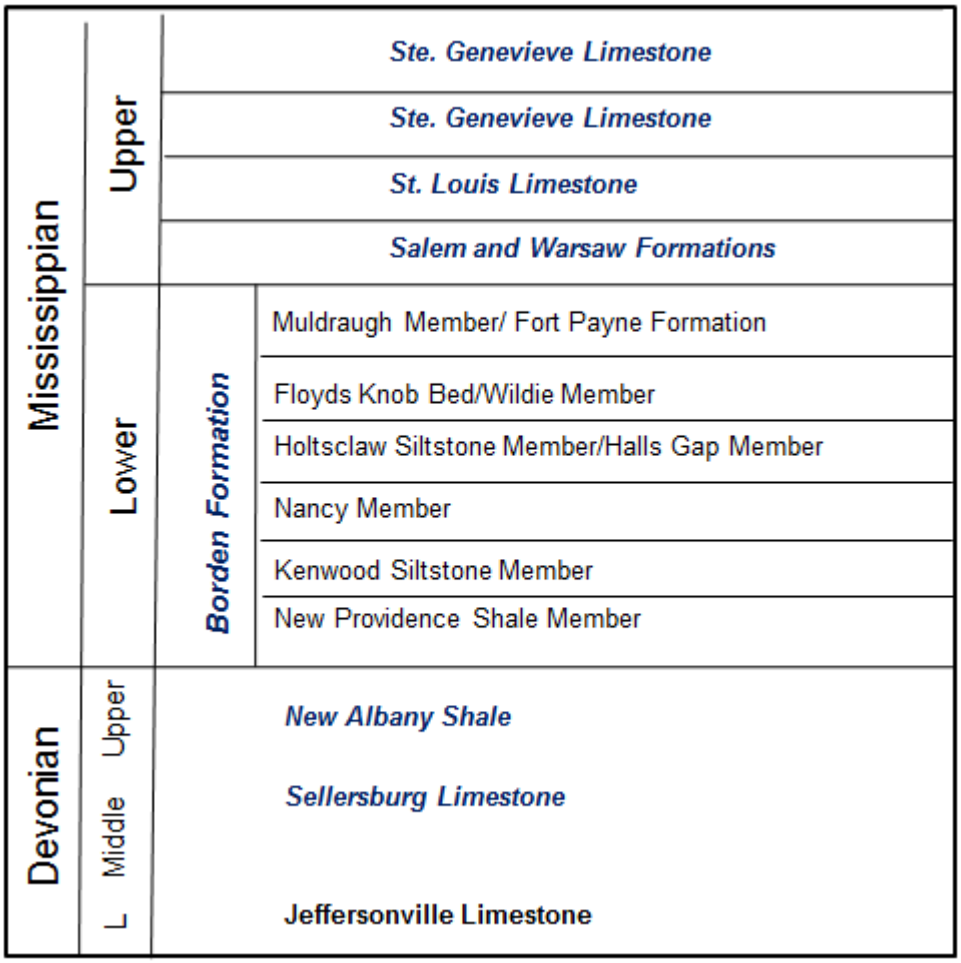

Figure 3.3. Stratigraphy of Devonian and Mississippian units. Blue bolded, italicized units were sampled.

Classification

Three broad lithologic groups were used to identify the gross lithology, and then subsequently further subdivided using visual properties and simple diagnostic tests: a carbonate group, a siliciclastic group, and an interbedded group (a combination of siliciclastic and carbonate). After this initial grouping based on lithology was complete, property arrays were used to further classify the sample set. The carbonate and interbedded groups made up the majority of the samples, which were further grouped or subdivided using property arrays focusing on one property at a time (grain size, percentage of shale, percentage of carbonate components, etc.).

The most easily recognizable and therefore primary property of interest for the limestone group was grain size. The limestone samples were laid out in arrays in order of fine to coarse grain size. A boundary was made at the transition in the array from fine-grained to coarse-grained, and

samples were grouped accordingly. The same procedure was applied for the interbedded limestone and shale group, with the property of interest being the percentage of shale in each sample (Figure 2.1). Boundaries were defined based on percentages of shale that could be macroscopically summarized (visual estimates of percentage of shale). An array was created for interbedded limestone and shale focusing on the percentage of carbonate components. After all properties of interest had been defined and explored by using arrays, the dominant classification categories were apparent.

All components of the carbonate samples effervesced with HCl; however, the strength of the reaction was used to classify samples as either dolostone (weak reaction to HCl—barely visible effervescence) or limestone (strong reaction to HCl—very visible effervescence). Limestone specimens were then grouped based on homogeneity, separating massive looking samples from those with conspicuous streaks, layers, or other masses of contrasting appearance. Homogenous samples were classified as fine- or coarse-grained. Fine-grained samples (Figure 3.4) were all massive, with some having mosaic-like cracks or styolites. Coarse-grained limestone samples (Figure 3.5) were more variable than fine-grained samples and less homogeneous. Grain composition varied from fossil fragments to carbonate mineral components (calcite crystals). Some homogeneous samples appeared layered, and the color ranged from dark to light.

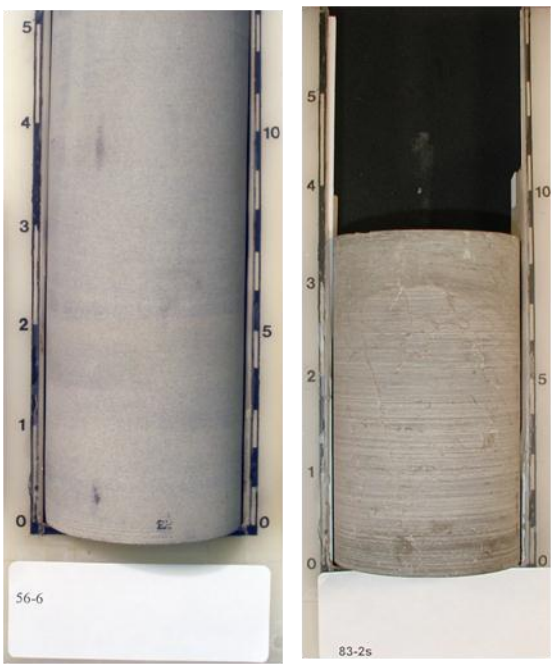

Figure 3.4. Fine-grained homogeneous limestone samples. Massive (56-6) and mosaic/styolite (83-2s) fabric representations.

Figure 3.5. Coarse-grained homogeneous limestone. Fossil fragment grains (25-7), predominantly calcium carbonate composition (78-1s), layered (85-8s), dark (68-3s), and light (78-1s) representations.

Heterogeneous limestone specimens (Figures 3.6–3.7) were divided into three main groups: nodular, streaked, and a miscellaneous heterogeneous group. Nodular samples (Figure 3.6)

initially appeared to be interbedded limestone and shale; however, the dark matter surrounding the carbonate nodules was carbonate, not siliciclastic. The light-colored carbonate components were composed of both fossil fragments and fine- and coarse-grained limestone. Streaked limestone samples (Figure 3.6) were predominantly limestone with very thin streaks that were most likely shale. Streak composition could not be confirmed with HCl because the streaks were thin and next to highly reactive calcium carbonate; however, these specimens were both coarse- and fine-grained (Figure 3.6). The unclassified heterogeneous group was very diverse. Some of these samples were bioturbated, and a few had calcite vugs (Figure 3.7) and were very porous. Some specimens appeared to be predominantly shale with fossil fragments; however, the dark matter surrounding the carbonate components reacted strongly to HCl and was therefore determined to be limestone (Figure 3.7). Some of the samples in this group were layered (Figure 3.7). There were not enough specimens in this group to warrant a more refined classification.

Figure 3.6. Heterogeneous limestone. Nodular (1-7), streaked (32-6 +s), coarse-grained (51-4), and fine-grained (49-1) representations.

Figure 3.7. Heterogeneous limestone. Bioturbated (47-2s), vuggy (65-3s), shaly limestone (40-5), and layered (84-3s) representations.

Siliciclastic samples were classified as shale, siltstone, or sandstone. Shale samples (Figure 3.8.) were subdivided based on color, bedding, and composition. Samples were either black or dark gray. All black shale samples were massive and appeared to be compositionally the same. Some dark gray samples were massive, whereas others were grain-oriented (noticeable because of weathering patterns). Some grain-oriented samples were very fissile (Figure 3.9) and broke along parallel planes. A few of the dark gray shale samples were sandy or silty (Figure 3.8.). Siltstone samples (Figure 3.10) had relatively distinct sandy layers, and many of the siltstones sampled appeared to be bioturbated. All of the siltstone samples were dark gray. Sandstones sampled were all homogenous, relatively light in color, and fine-grained (Figure 3.10).

Interbedded carbonate and siliciclastic samples (Figure 3.11) were all predominantly limestone with shale layers. Carbonate components included fossil fragments, limestone fragments (both fine- and coarse-grained), and a combination of both. Most samples were bioturbated.

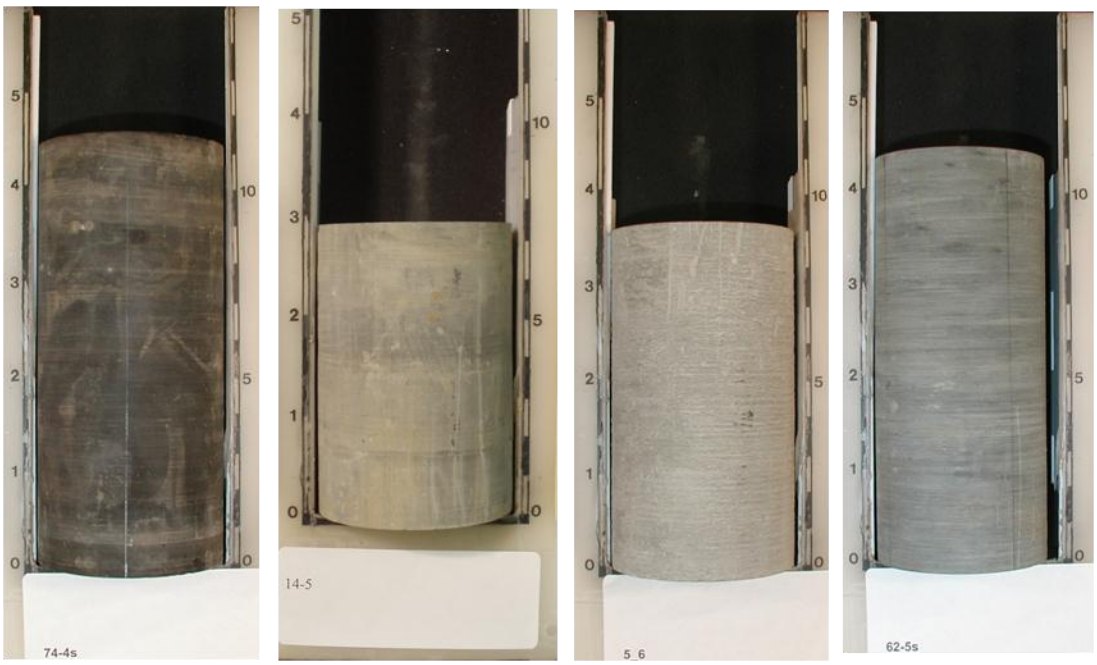

Figure 3.8. Shale. Black (74-4s), massive dark gray (14-5), grain-oriented dark gray (5-6), and sandy shale (62-5s) representations.

Figure 3.9. Fissile shale.

Figure 3.10. Siltstone and sandstone. Sandy/streaked layered siltstone (69-6s) (62-2s), bioturbated siltstone (71-2s) representations, along with sandstone (52-spt-1).

Figure 3.11. Interbedded limestone and shale. Fossil-fragment dominated (26-5s), limestone-dominated (16-19), and both fossil fragment and limestone (27+1+s) representations.

A flow chart of the megascopic classification was created (Figure 3.12) in order to lead practitioners to classifying core samples based on the classification that was defined by the arrays and to ensure repeatability. Samples were grouped into one of 13 categories (Table 3.1). Each category had a corresponding abbreviated classification.

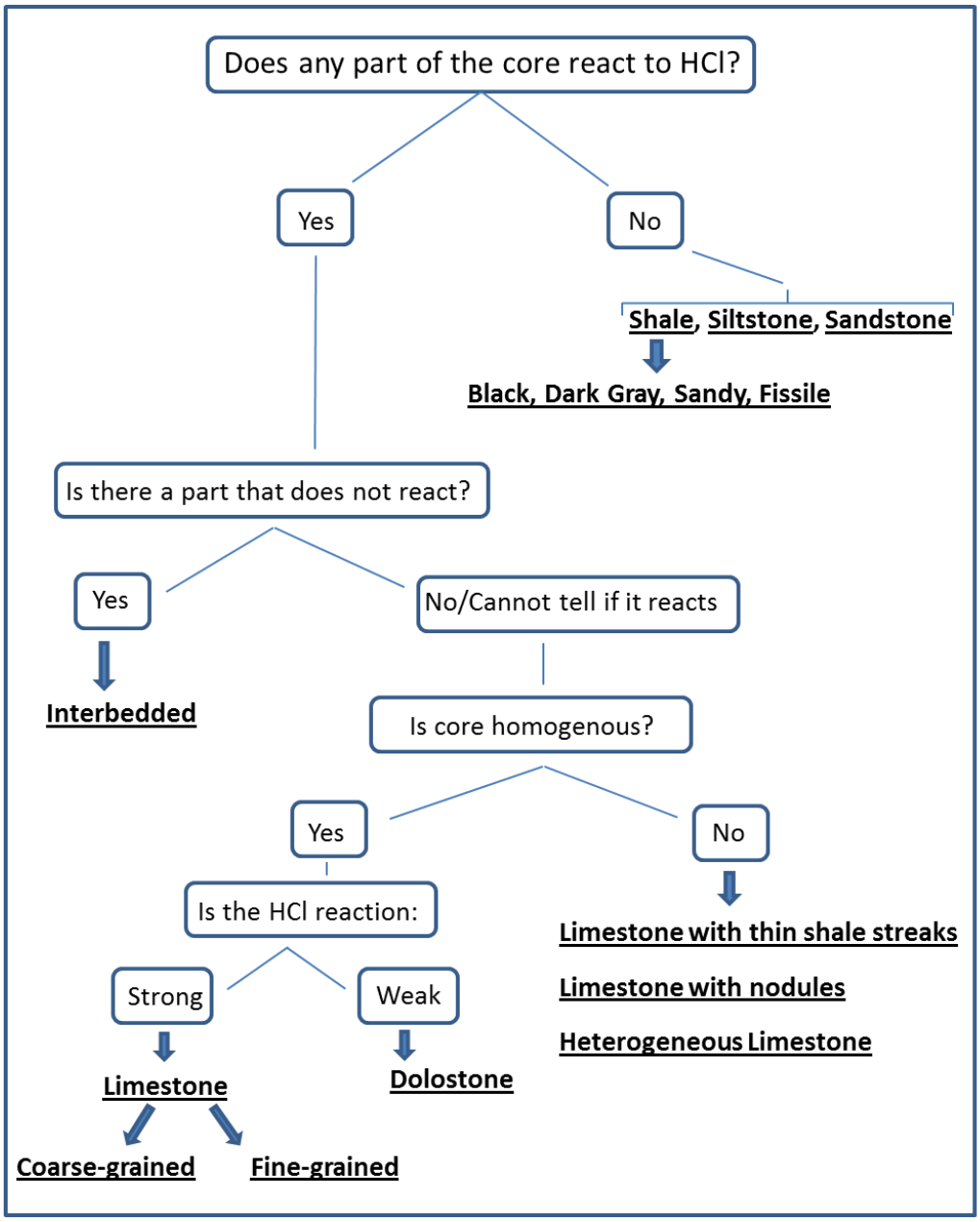

Figure 3.12. Classification flow chart.

Table 3.1. Abbreviated classification table.

Lithology	Abbreviated Classification
Dolostone	DOL
Limestone, coarse-grained	LS CG
Limestone, fine-grained	LF FG
Limestone, heterogeneous	LS HET
Limestone, nodular	LS NOD
Limestone, with thin shale streaks	LS TSS
Interbedded	INT
Shale, black	SH BL
Shale, gray	SH GRY
Shale, sandy	SH SDY
Shale, fissile	SH FS
Siltstone	SILT
Sandstone	SS

Sample Set

Of the 771 samples taken, 115 representative samples were prepared for further testing. Fifty-six percent of the prepared samples were carbonate, 11 percent were interbedded, and 33 percent were siliciclastic (Figure 3.13).

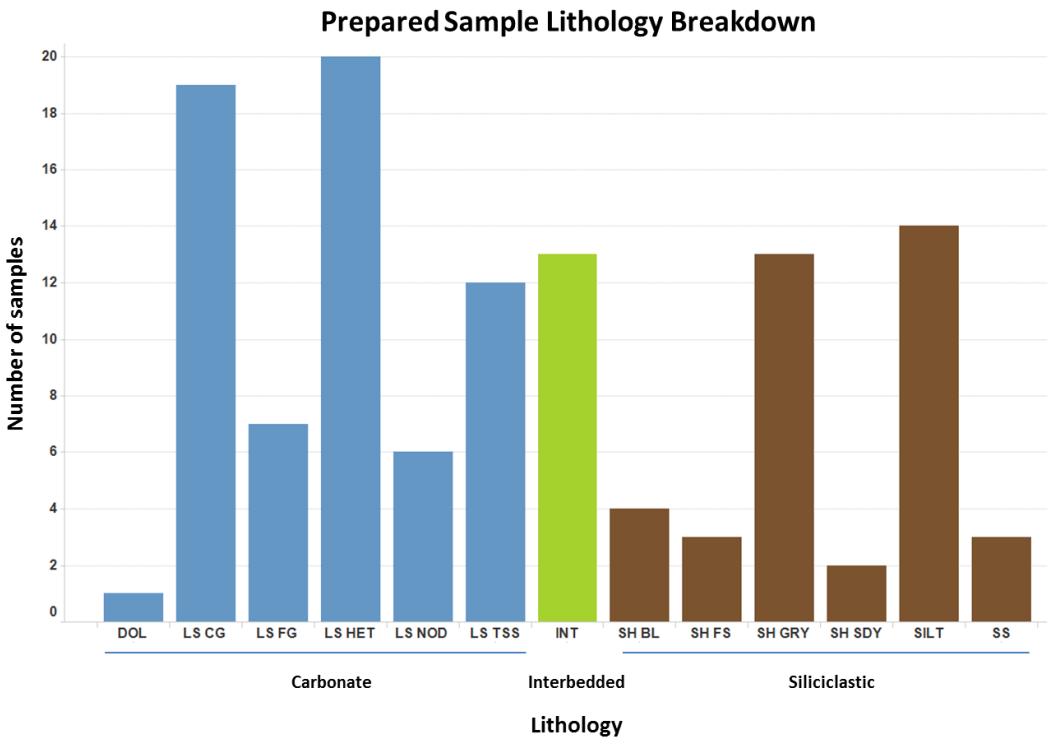

Figure 3.13. Population distribution of prepared sample lithologies.

Rock Density

The density of the specimens ranged between 2.29 g/cm^3 and 2.89 g/cm^3 (Figure 3.14). The bulk of the siliciclastic rocks had similar densities, ranging between approximately 2.4 g/cm^3 and 2.7 g/cm^3, with the exception of black shale, which ranged between 2.29 g/cm^3 and 2.35 g/cm^3. The majority of carbonate rocks ranged between approximately 2.55 g/cm^3 and 2.7 g/cm^3, with the exception of heterogeneous limestone, which had a more dispersed variation between 2.42 g/cm^3 and 2.69 g/cm^3. The majority of the interbedded limestone and shale samples mimicked the density of the carbonate specimens, with a range between 2.58 g/cm^3 and 2.70 g/cm^3. There were relatively few outliers in all general lithologic groups.

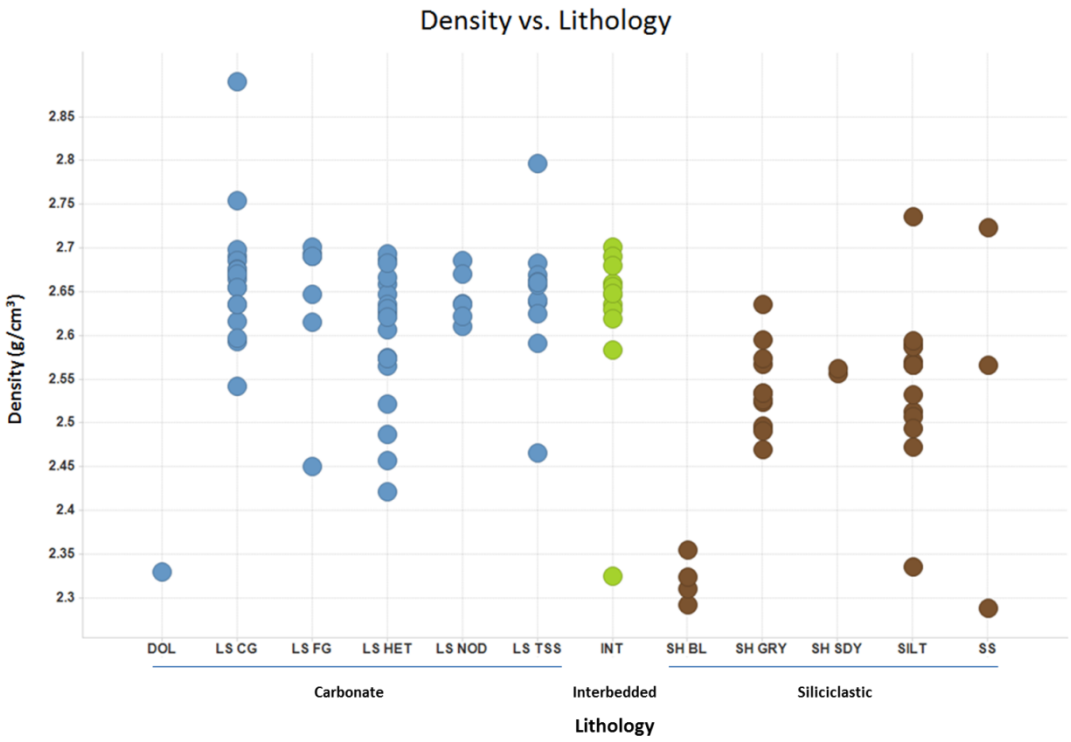

Figure 3.14. Density values displayed by lithology.

Density Discussion

Specimen density results are comparable to the densities of similar sedimentary rocks (Table 3.2). Density results can lead to broad conclusions about mineral composition and pore space. For example, the density results for the black shale samples are lower than those for other lithologies because of the black shales' high organic content. Limestone results tend to be tightly clustered between 2.6 g/cm^3 and 2.7 g/cm^3, comparable to the value for calcite (2.72 g/cm^3), which could suggest low porosity for most samples. The spread of the heterogeneous limestone category might be attributed to the presence of argillaceous/shaly limestone (Figure 3.7) and also high-porosity/vuggy limestone (Figure 3.7). The density of the interbedded limestone and shale is more like that of limestone, which was unexpected. This may be attributed to the amount of limestone in these samples (they are predominantly limestone; see Figure 3.11); however, the presence of siliciclastics should reduce the overall density. A difference in shale mineralogy in the interbedded samples compared with the siliciclastic samples could also affect

the density. The overlap of density values based on lithology is significant, because it shows density alone would be difficult to use to predict material behavior.

Table 3.2. Density of common rocks types (Burger, 1992).

Rock Type	Density (g/cm^3)
Limestone	2.5–2.8
Dolostone	2.3–2.9
Shale	2.0–2.7
Sandstone	2.0–2.6
Clay minerals	2.5–2.8
Calcite	2.72
Quartz	2.65

Sonic Velocity of Samples

Compression Waves

Compression-wave velocity for all lithologies ranged between 540 m/s and 6,451 m/s (Figure 3.15). The carbonate rocks generally had higher values compared to siliciclastic rocks. The bulk of the carbonates ranged between approximately 4,000 m/s and 6,200 m/s, with the exception of heterogeneous limestone, which varied between 540 m/s and 6,161 m/s. Most of the samples of limestone with thin shale streaks had relatively higher densities than other carbonate types did, ranging between approximately 4,500 m/s and 5,700 m/s, and the density range for nodular limestone was lower than for the other carbonates, between 2,476 m/s and 5,124 m/s. The siliciclastic units had generally lower values than the carbonate rocks did, with most ranging between 1,500 m/s and 4,000 m/s. Siliciclastic rocks showed a distinct grain size/velocity relationship of higher velocity with increasing grain size. The black shale had significantly lower values compared to the other siliciclastic rocks, ranging between 559 m/s and 1,559 m/s. The dark gray shale fell in two general clusters, the lower ranging between 1,266 m/s and 1,794 m/s and the upper between 2,341 m/s and 3,102 m/s. The siltstone specimens had the largest spread of all the siliciclastic rocks, ranging between 1,826 m/s and 3,977 m/s. The interbedded limestone and shale samples had a narrow range of velocity between 3,029 m/s and 6,044 m/s, comparable to other limestone lithologies. The heterogeneous limestone group

showed the greatest spread of all lithologies. Outliers were present in all general lithology groups.

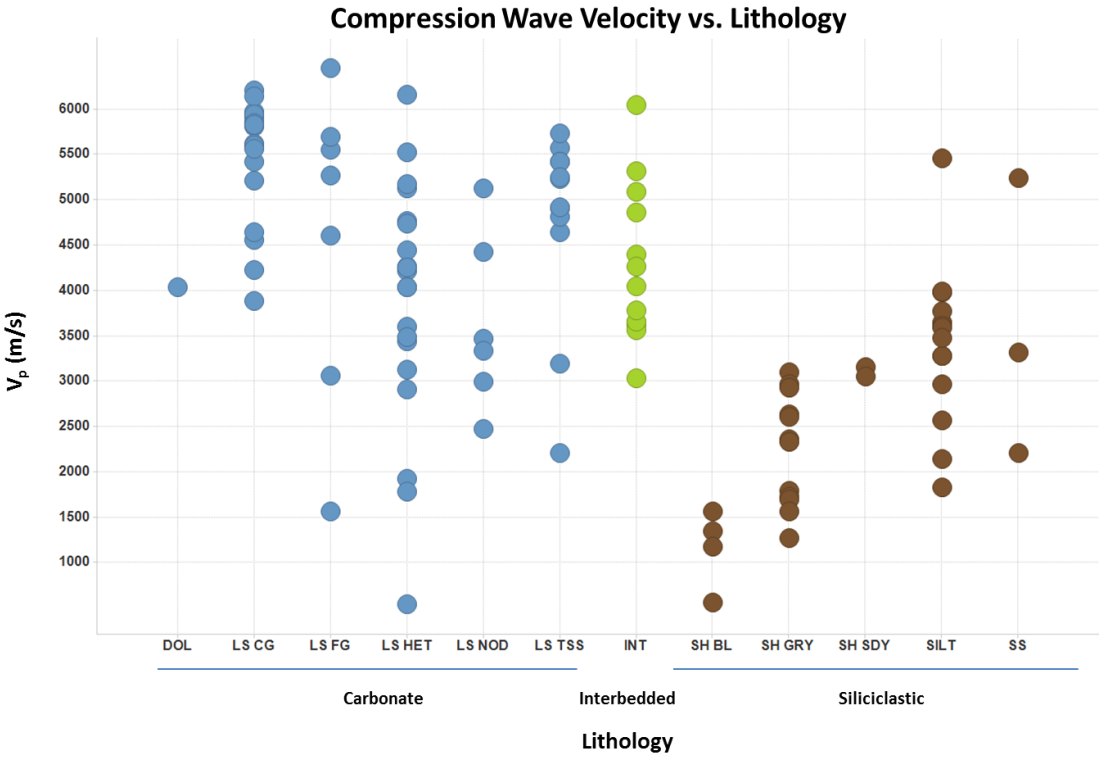

Figure 3.15. Compression-wave velocity values displayed by lithology.

Shear Waves

The bulk of the shear wave velocity results ranged from approximately 700 m/s to 3,300 m/s (Figure 3.16). Shear wave results were similar to compression wave results; however, the variation in shear wave velocity results was generally smaller. The majority of the results for carbonate specimens ranged between 2,000 m/s and 2,800 m/s. The exception was the heterogeneous limestone, which had a greater range between 895 m/s and 2,802 m/s, and the nodular limestone, which was lower than the other carbonate units and ranged between 1,562 m/s and 2,123 m/s. The siliciclastic specimens' values were generally lower than the carbonate sample values. The bulk of the siliciclastic specimens ranged between 800 m/s and 2,300 m/s. The black shale values were the lowest, ranging between 868 m/s and 1,197 m/s. The dark gray shale results plotted in two distinct clusters, similar to compression wave velocity results, the lowest ranging between 1,093 m/s and 1,381 m/s, and the uppermost population ranging between 1,972 m/s and 1,800 m/s. The siltstone specimens had the largest spread of all the

siliciclastic rocks, ranging between 1,367 m/s and 2,582 m/s. The results for the interbedded samples were similar to those of the average carbonate rocks, the bulk of which ranged between 1,925 m/s and 2,628 m/s. There were few outliers in each general lithologic group.

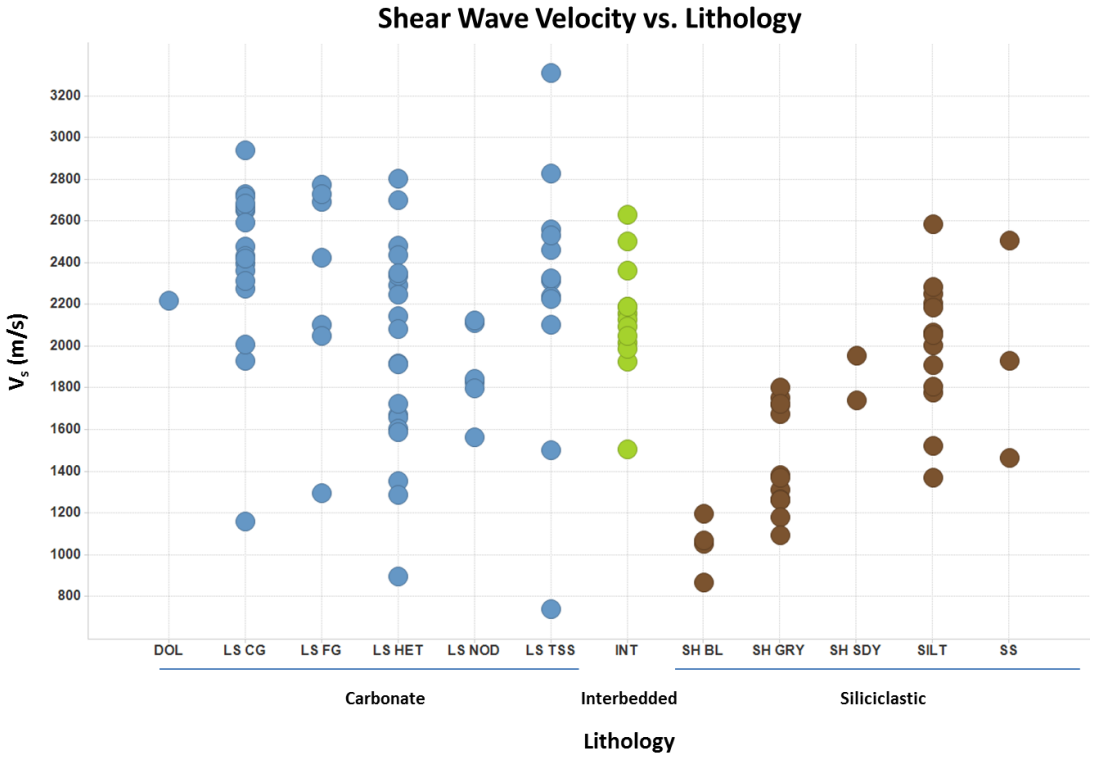

Figure 3.16. Shear wave velocity values displayed by lithology.

Velocity Discussion

Velocity results for the sample set are comparable to those for similar common sedimentary rock types (Table 3.3). Shear wave values are expected to be about half of compression wave values for sedimentary rocks (Burger, 1992). Shear wave velocity as a percentage of compression wave velocity was calculated (Table 3.4), and the results are consistent in that most averaged shear wave values are roughly half of compression wave values. The exception to this was black shale.

The ratio of compression waves to the velocity of shear waves (V_p/V_s) can be used to interpret geophysical field data (Wilkens et al., 1984) and is correlative to sedimentary lithology (Tatham, 1982). The ratio is more useful as a correlative tool for carbonate lithologies than for clastic lithologies because porosity and clay content can affect the V_p/V_s parameter (Johnston and

Christensen, 1993; Tatham, 1982). Pickett (1963) was the first to suggest the correlation between V_p/V_s ratio and rock type, and defined the following lithologies and ratios: limestone, 1.9; dolomite, 1.8; and sandstone, 1.6 to 1.75. Results for specimens tested in this study are comparable to these ratios (Table 3.4).

Table 3.3. Elastic coefficients and velocities for selected common rocks. Adapted from Burger (1992).

Rock Type	Density	Young's Modulus	Poisson's Ratio	V_p (m/s)	V_s (m/s)	V_p/V_s	V_s as $\%V_p$
Shale (AZ)	2.67	0.120	0.040	2,124	1,470	1.44	69.22
Siltstone (CO)	2.5	0.130	0.120	2,319	1,524	1.52	65.71
Limestone (PA)	2.71	0.337	0.156	3,633	2,319	1.57	63.84
Limestone (AZ)	2.44	0.170	0.180	2,750	1,718	1.6	62.47
Sandstone (WY)	2.28	0.140	0.060	2,488	1,702	1.46	68.42

Table 3.4. Average elastic coefficients and velocities for each lithologic group in the study sample set.

Lithology	Density ρ	Young's Modulus *E*	Poisson's Ratio μ	Vp (m/s)	Vs (m/s)	Vp/Vs	Vs as %Vp
Sandstone	2.53	0.270	0.235	3,591	1,967	1.77	54.79
Siltstone	2.55	0.253	0.176	3,399	2,005	1.67	59.00
Shale, sandy	2.56	0.212	0.216	3,101	1,847	1.69	59.57
Shale, gray	2.53	0.119	0.032	2,255	1,445	1.54	64.10
Shale, black	2.32	0.044	–0.127	1,159	1,047	1.12	90.33
Limestone with thin shale streaks	2.65	0.376	0.300	4,775	2,262	2.42	47.37
Limestone, nodular	2.64	0.246	0.287	3,637	1,877	1.91	51.62
Limestone, heterogeneous	2.60	0.286	0.347	3,877	1,974	1.91	50.91
Limestone, fine-grained	2.64	0.378	0.185	4,599	2,295	1.94	49.91
Limestone, coarse-grained	2.67	0.439	0.370	5,476	2,426	2.32	44.30
Interbedded	2.63	0.319	0.306	4,255	2,134	2.00	50.15
Dolostone	2.33	0.295	0.284	4,040	2,219	1.82	54.93

Effect of Density on Velocity Discussion

The relationship between density and velocity is normally expected to be approximately linear. The time it takes for a wave to travel through rock depends on the density of the minerals forming the rock, the porosity of the rock, and the anisotropic arrangement of the material forming the minerals making up the rock (Gaviglio, 1989). In this study, as density increased, the velocity increased for both compression (Figure 3.17) and shear waves, but with significant

variation (note overall coefficient of determination (R^2) value of 0.428). The deviation from a completely linear trend can likely be attributed to the anisotropic arrangement of the minerals in the samples as well as to some samples having vuggy porosity.

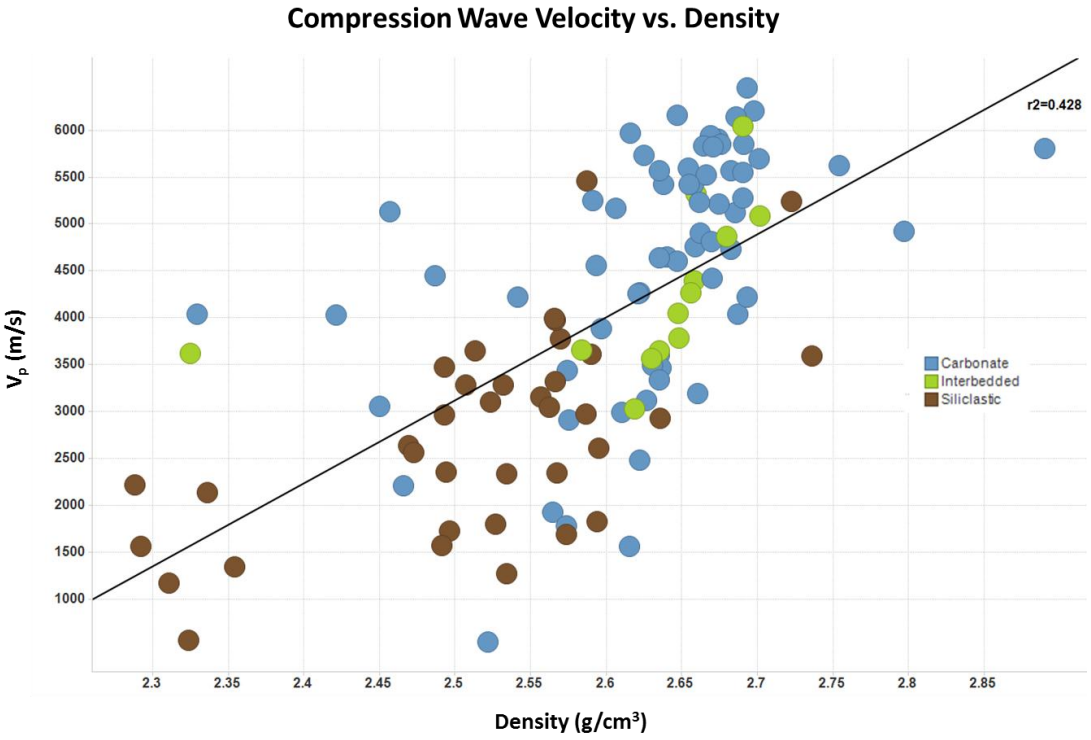

Figure 3.17. Compression wave velocity versus density.

Velocity/density graphs were created for each lithologic category, and the coefficient of determination (R^2) was calculated. When comparing density versus shear wave velocity (Table 3.5), black shale and sandstone had the highest R^2 values in the siliciclastic group, whereas fine-grained limestone, nodular limestone, and limestone with thin shale streaks had the greatest R^2 values (from greatest to least, respectively) among the carbonates.

Table 3.5. Density and shear wave velocity trend analyses.

Lithology	No. of Samples	R^2, All Data	R^2, Outliers Removed	No. of Outliers
LS CG (Limestone, coarse-grained)	19	0.002	0.118	2
LS FG (Limestone, fine-grained)	7	0.272	0.94	1
LS HET (Limestone, heterogeneous)	20	0.013	0.38	3
LS NOD (Limestone, nodular)	6	0.746	–	0
LS TSS (Limestone, thin shale streaks)	12	0.013	0.632	3
INT (Interbedded)	13	0.113	0.417	2
SH BL (Shale, black)	4	0.94	–	0
SH GRY (Shale, gray)	13	0.054	–	0
SH SNDY (Shale, sandy)	2	–	–	–
SILT (Siltstone)	14	0.181	0.258	3
SS (Sandstone)	3	0.953	–	0
DOL (Dolomite)	1	–	–	–
ALL LITHOLOGIES	114	0.252	–	–

For density versus compression wave velocity analyses (Table 3.6), sandstone had the highest R^2 value (0.905) of the siliciclastic rocks; however, this may be attributed to the small number of sandstone samples (three). The majority of carbonates had higher values, with nodular limestone having the highest at 0.909 and fine-grained limestone having the second-highest at 0.859.

Table 3.6. Density and compression wave velocity trend analyses.

Lithology	No. of Samples	R^2, All Data	R^2, Outliers Removed	No. of Outliers
LS CG (Limestone, coarse-grained)	19	0.303	0.512	1
LS FG (Limestone, fine-grained)	7	0.444	0.859	1
LS HET (Limestone, heterogeneous)	20	0.069	0.566	3
LS NOD (Limestone, nodular)	6	0.909	–	0
LS TSS (Limestone, thin shale streaks)	12	0.283	0.428	1
INT (Interbedded)	13	0.213	0.637	1
SH BL (Shale, black)	4	0.043	–	0
SH GRY (Shale, gray)	13	0.027	–	0
SH SNDY (Shale, sandy)	2	–	–	–
SILT (Siltstone)	14	0.15	0.299	3
SS (Sandstone)	3	0.905	–	0
DOL (Dolomite)	1	–	–	–
ALL LITHOLOGIES	114	0.428		

Other Elastic Constants

Poisson's Ratio

Poisson's ratio for all specimens ranged from –1.62 to 1.29, with the bulk of the values mainly in the –0.2 to 0.05 range (Figure 3.18). The bulk of the carbonate values (–0.04 to 0.49) were higher than the siliciclastic values (–0.15 to 0.36). Black shale had the largest variation, ranging from –1.62 to 1.19. Interbedded specimens had values similar to those for carbonates. There were five significant outliers.

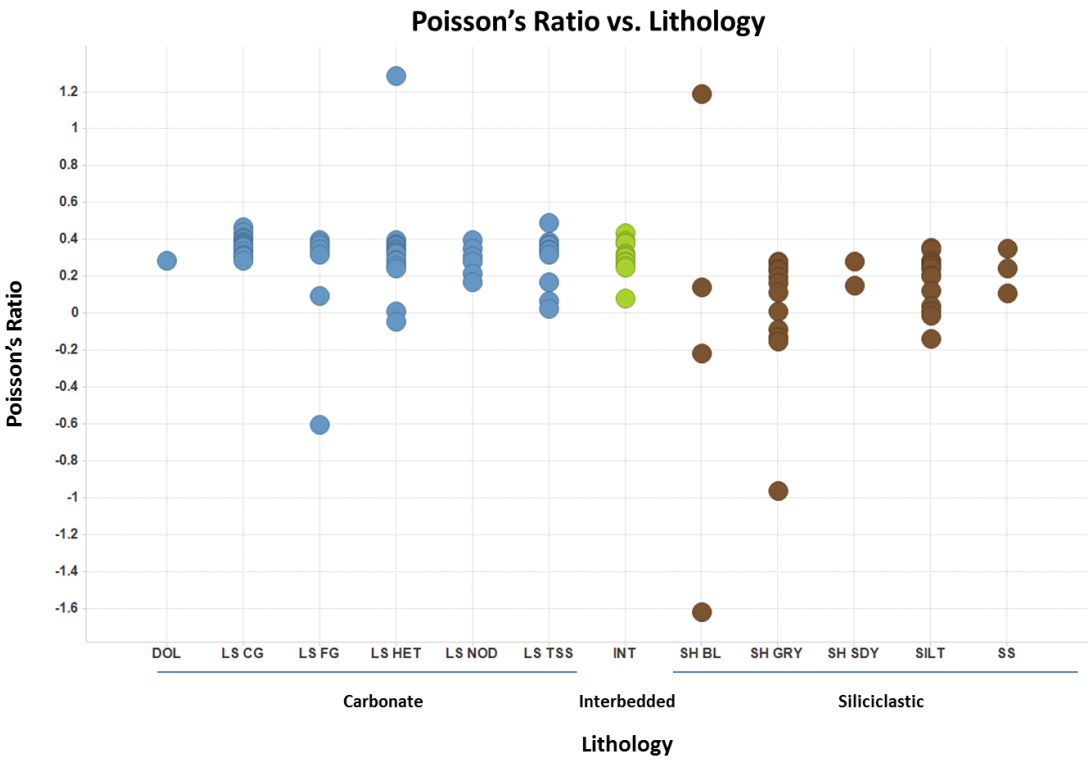

Figure 3.18. Poisson's ratio results displayed by lithology.

When the outliers were removed, the trends associated with lithology could be better understood (Figure 3.19). Siliciclastic values were generally more varied than those for carbonates and reflect the two distinct velocity groups shown in previous sections. Two carbonate populations were also obvious. The bulk of the first population varied little and was clustered between 0.25 and 0.4, with the exception of coarse-grained limestone, which had higher values (0.29–0.47). The second population was more varied and included one to three samples from all of the other carbonate groups, with the exception of coarse-grained limestone, and ranged between –0.04 and 0.22.

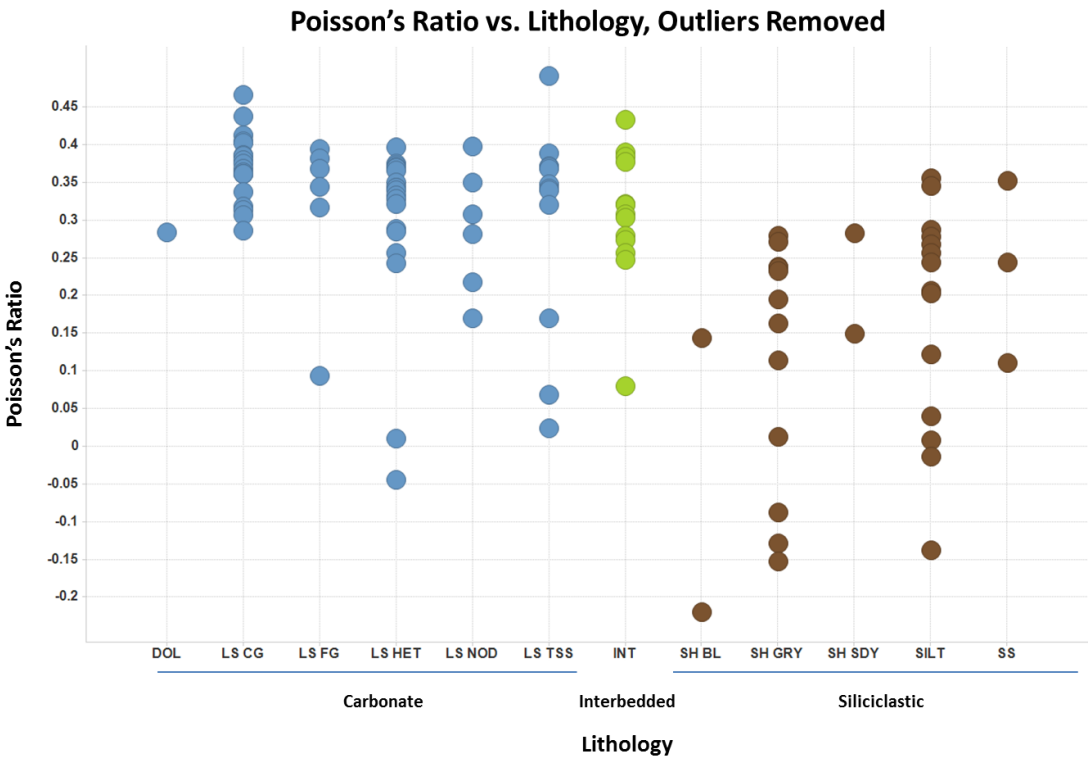

Figure 3.19. Poisson's ratio versus lithology (with outliers removed).

Shear Modulus

Shear modulus values ranged between 1.46 GPa and 28.39 GPa (Figure 3.20). The siliciclastic values (1.78 GPa–17.26 GPa) were lower than the carbonate values (1.46 GPa–28.39 GPa) and interbedded values (6.02 GPa–18.59 GPa). Black shale values were low (1.78 GPa–3.29 GPa). There were two populations of gray shale values, one of which ranged between 3.03 GPa and 4.76 GPa and the other between 6.91 GPa and 8.55 GPa. Both the siltstone (4.85 GPa–17.26 GPa) and sandstone (4.91 GPa–17.10 GPa) values had larger spreads than those for the other siliciclastic specimens. The coarse-grained limestone ranged between approximately 10 GPa and 20 GPa. Fine-grained limestone (4.39 GPa–20.81 GPa), heterogeneous limestone (2.02 GPa–20.78 GPa), and limestone with thin shale streaks (1.46 GPa–28.39 GPa) were all quite variable; limestone with thin shale streaks had the greatest spread. The interbedded samples stayed within the carbonate specimen range.

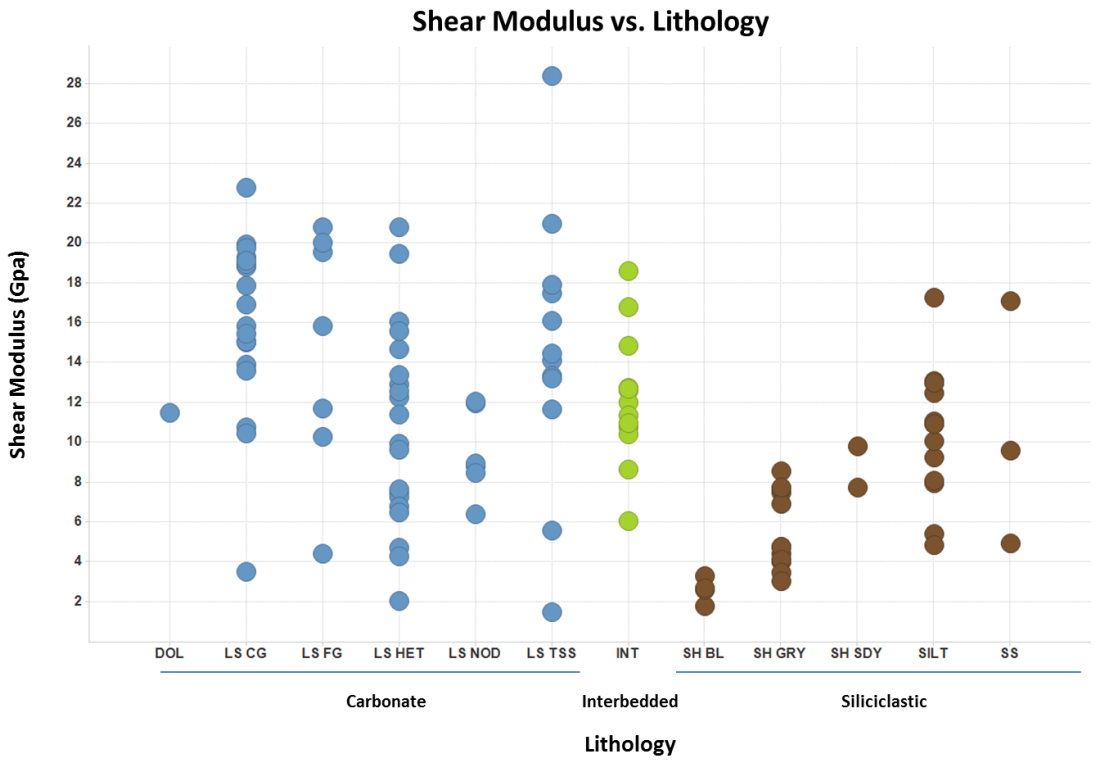

Figure 3.20. Shear modulus versus lithology.

Young's Modulus

The values for Young's modulus ranged between 0.23 GPa and 66.42 GPa (Figure 3.21). The overall trends were similar to the shear modulus trends. Siliciclastic values (0.23 GPa–46.79 GPa) were lower than carbonate values (3.46 GPa–66.42 GPa) and interbedded values (17.26 GPa–51.45 GPa). The black shale values were the lowest of the siliciclastic values, ranging between 4.06 GPa and 11.61 GPa (one negative black shale value was discarded). Both siltstone and sandstone had large spreads ranging between 8.36 GPa and 46.79 GPa and between 10.89 GPa and 46.24 GPa, respectively. The carbonate specimen results were in a similar range and relatively spread out, with the exception of the results for nodular limestone. The values for these specimens were lower and ranged between 15 GPa and 33.40 GPa. The limestone with thin shale streaks had the greatest spread (4.36 GPa–66.42 GPa) and the values for coarse-grained limestone, with the exception of one lower value at 10.18 GPa, was somewhat higher than the other carbonate values and less spread out, ranging between 27.55 GPa and 59.59 GPa.

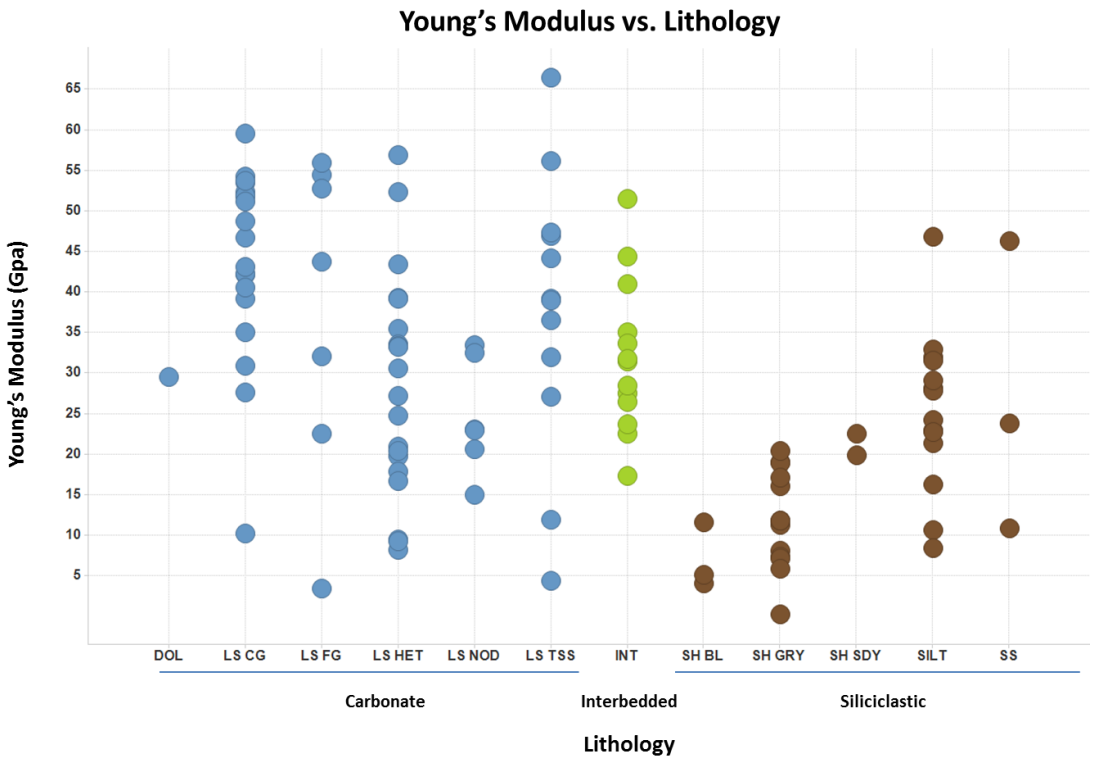

Figure 3.21. Young's modulus results displayed by lithology.

Elastic Constants Discussion

The elastic constant results were generally bi- and multimodal for most lithologies; therefore, summary statistics were not utilized when analyzing the result data. Poisson's ratio is expected to range between –1 and 0.5, with most values of isotropic materials ranging between 0 and 0.5. Negative values are typically associated with anisotropic materials. Common values for Poisson's ratio by rock type can be seen in Table 3.7 (Gercek, 2007).

Table 3.7. Common values for Poisson's ratio (Gercek, 2007).

Lithology	Poisson's ratio range
Dolomite	0.1–0.35
Limestone	0.1–0.325
Sandstone	0.05–0.4
Shale	0.05–0.325
Siltstone	0.0125–0.35

These values are comparable to the sample set results, with the exception of the lower values for sandstones, shales, and siltstones. Although there were not numerous negative values, the majority of the negative values were in the siliciclastic group. The heterogeneous limestone results are less variable than those of the siliciclastic groups, which is unlike other results (e.g., density and velocity). The sample set results do, however, mimic Gercek's results, with the siliciclastics having the greater ranges.

Shear modulus and Young's modulus values behaved similarly to each other. Siliciclastic values increased with increasing grain size. Both limestone with thin shale streaks and heterogeneous limestone values were more variable. This indicates that bedding plays a more important role for these elastic constants. Many of the Young's modulus values for the sample set were not within the spread of comparable values according to West (1994) (Table. 3.8). The sandstone samples fell within a comparable range to West's values, whereas the dolomite sample is lower. With only one dolomite sample, however, a clear comparison cannot be made. In relation to West's values, many of the shale sample values are lower and many of the limestone samples are higher. This may have to do with the broad, highly anisotropic sample set of this study.

Table. 3.8. Young's modulus values. Modified from West (1994).

Lithology	Young's Modulus (GPa)
Sandstone	4.7–76.5
Shale	9.7–33.8
Limestone	19.3–47.6
Dolomite	37.9–80.0

Unconfined Compressive Strength

Twenty-nine samples were tested for uniaxial compressive strength. Results were calculated in English units (psi) as opposed to the International System of Units (SI) because English units for this parameter are more widely used by geotechnical engineers and geologists. Interbedded and siliciclastic samples were tested, but the bulk of the testing was conducted on carbonate specimens (Figure 3.22). Coarse-grained limestone tested the strongest, with values ranging between 10,000 psi and 16,000 psi. One fine-grained sample tested very high, with a value of 16,160 psi; however, all other carbonates tested lower. The heterogeneous limestone had the greatest variation, with results ranging between 3,260 psi and 11,270 psi. Two black shale samples tested high, with values over 13,000 psi. Gray shale values were lower than values for black shale and the siltstone sample had the lowest of all siliciclastic values. Two of the three interbedded samples were clustered between 7,000 and 8,000 psi, whereas one sample tested the highest of all samples, at over 18,000 psi.

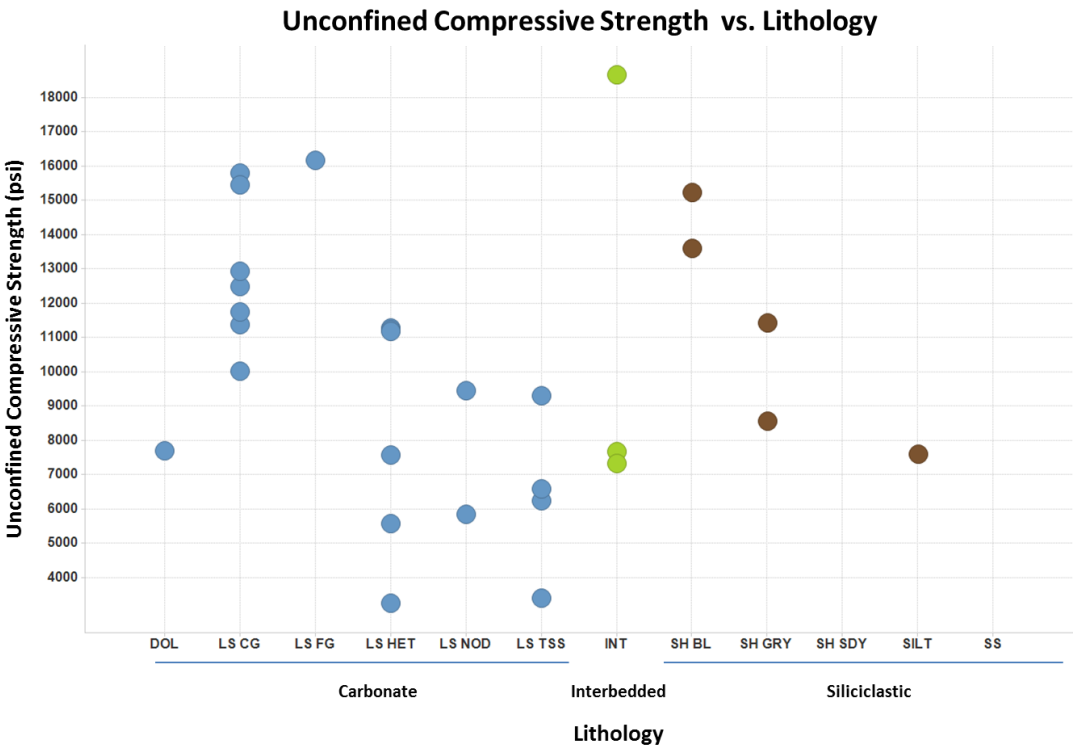

Figure 3.22. Unconfined compressive strength values displayed by lithology.

Unconfined Compressive Strength Discussion

The sample set values are comparable to compressive strength values for analogous sedimentary rocks (Table 3.9). The range of the values for general rocks types is quite large, however, making it difficult for this parameter to be useful alone. Homogeneity appears to be the dominant factor with regard to this parameter. The lowest values were in the heterogeneous, nodular, and thin shale-streaked limestone categories. Although the siltstone was within the normal range according to West (1994), values were low for that homogeneous rock type. The trend in siliciclastics is opposite that of velocity; the values increase as grain size decreases. Results could be affected by the uniaxial nature of the unconfined compression strength, in which strength is greater with increasing grain alignment parallel to bedding. The two black shale samples, for example, have high strength results. These results could lead to a false sense of rock strength.

Table 3.9. Compressive strength by lithology (West, 1994).

Lithology	Compressive Strength (psi)
Sandstone	2,780–23,600
Shale, general	1,390–13,900
Siltstone	4,120–7,290
Limestone	4,170–34,700
Dolomite	11,100–34,700

Unconfined Compressive Strength versus Velocity Discussion

The relationship between wave velocity and compressive strength is correlative with lithology in this study. Shear and compression wave velocity behaved similarly. As velocity increased, compressive strength increased for carbonate and interbedded samples (Figure 3.23). Siliciclastic sample results, however, displayed a completely different and less predictable trend. This might have been affected by the low number of siliciclastic samples tested. Yasar and Erdogan (2004) conducted a study in which a linear trend was found when relating compressive strength to compression wave velocity. Their samples were isotropic carbonates, however.

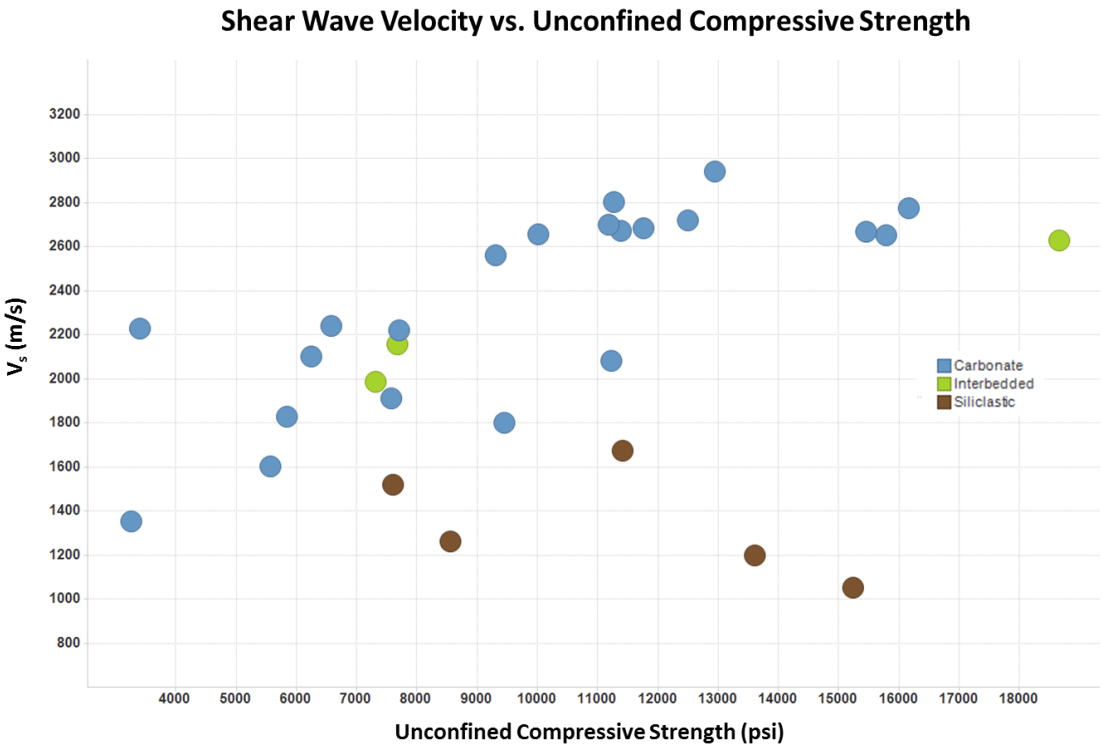

Figure 3.23. Shear wave velocity versus unconfined compressive strength.

Unconfined Compressive Strength versus Young's Modulus Discussion

A relationship exists between elastic moduli and strength. As strength increased, Young's modulus increased (Figure 3.24). The same trend was true for shear modulus. Some homogeneous lithologic groups—coarse-grained limestone, nodular limestone, and limestone with thin shale streaks—were clustered which supports the classification groupings. Material behavior for these groups will be easier to predict, whereas material behavior for heterogeneous groups will be more difficult to predict.

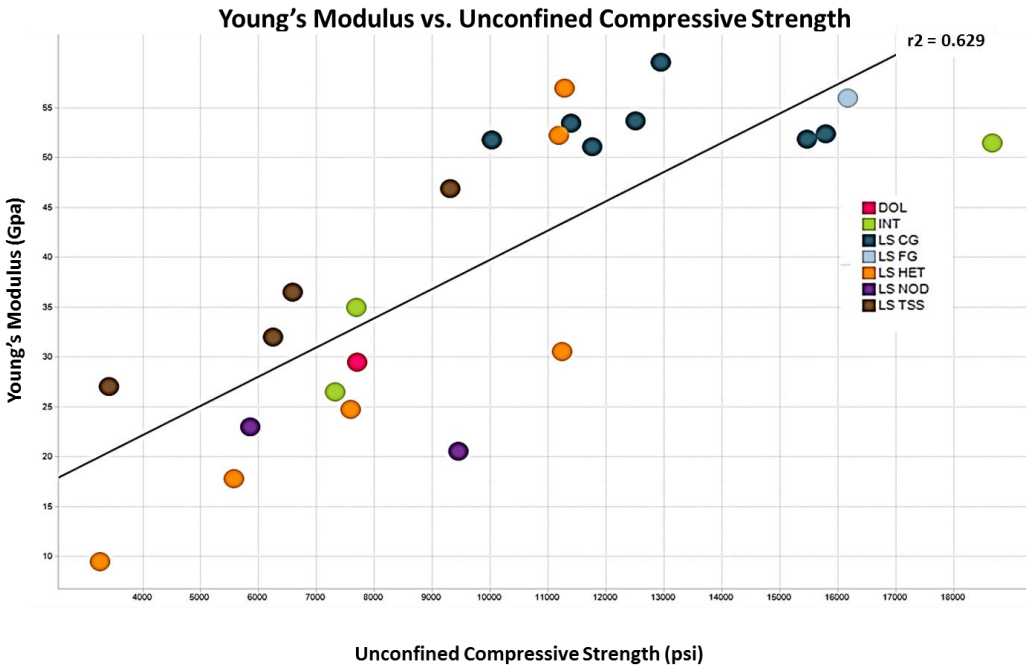

Figure 3.24. Young's modulus versus unconfined compressive strength.

Slake Durability

Eighteen specimens, most of which were shale, were tested for slake durability. The majority of the values were above 90 percent (Figure 3.24). Results were binary; they were either high or low. The black shale samples all had high values, above 95 percent. The gray shale results also indicated high values (above 89 percent), with one exception at 31 percent. Fissile shale specimens had consistently low values ranging between 34 and 41 percent. Several carbonates (one heterogeneous limestone, one nodular limestone, a limestone with thin shale streaks, and an interbedded sample) were tested, all resulting in values over 80 percent.

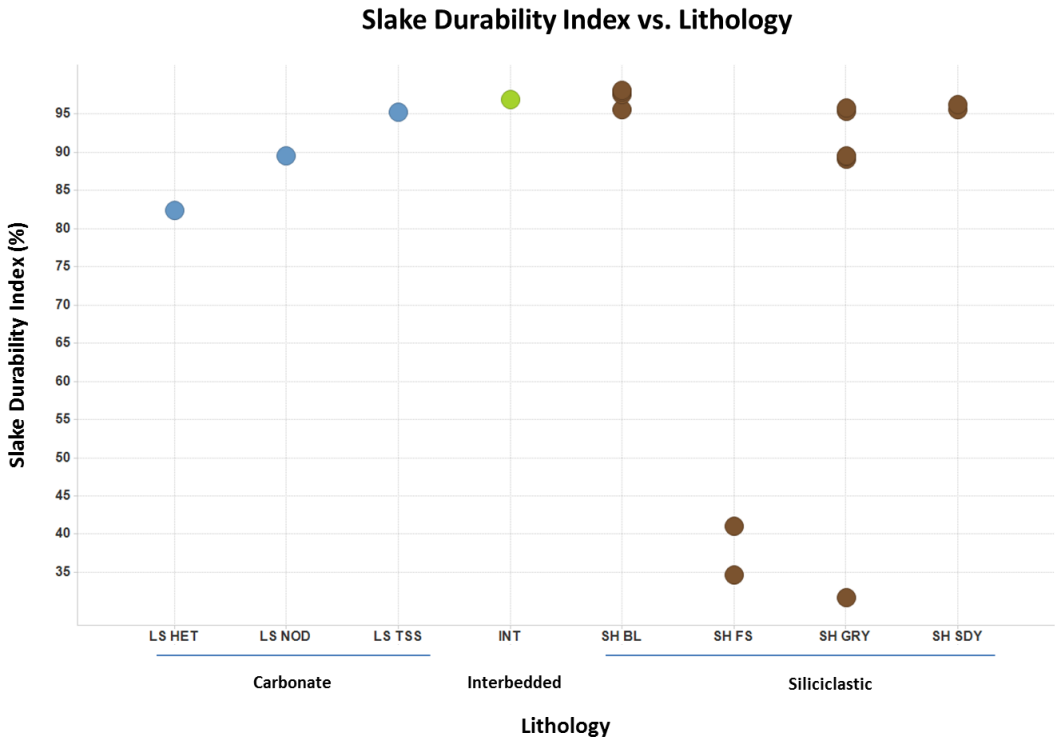

Figure 3.25. Slake durability index versus lithology.

Slake Durability Discussion

Slake durability sample set results were as expected. The only consistently weak values were found in all of the fissile shale samples. These samples appeared to be heavily weathered and the low value results were therefore expected. The low-value dark gray shale specimen looked similar to the other dark gray shale values, so its behavior is not consistent. This could be the result of a number of factors, including clay mineralogy, fabric differences, the degree of weathering, and the presence of carbonate minerals in some of the shale samples. Slake durability values in this study varied widely from statewide tests done in 2008–2010 (Table 2.1). Statewide testing indicated that 39 percent of samples were durable and 61 percent were nondurable. This indicates that the shale sampling in this study is incomplete and not representative.

CHAPTER 4: CONCLUSIONS

Sampling and Classification

The classification was created to provide an efficient field classification scheme. Hydrochloric acid was the only testing aid used, aside from visual characterizations, to ascertain lithologic composition; consequently, the number of categories is limited. The classification process was purposefully succinct in order to accommodate field work. A significant finding shows a sensitivity in rocks with shaly-appearing layers, which make up a significant proportion of the classification. Many of the samples were visually misleading in that some shalier-looking lithologies reacted to HCl and were carbonates. This could bias testing if these samples were categorized as interbedded samples as opposed to carbonate samples. A microscopic examination of each classified unit would better characterize samples, but would make field classification impossible. Nonetheless, the classification scheme was entirely successful as a means for obtaining representative samples and is well along the road to improving rock descriptions by geotechnical personnel.

This study differed from previous work correlating sonic velocity to elastic parameters in that no effort was made to restrict samples to homogeneous materials. Rock samples in this study varied widely, and the majority of them were heterogeneous. This caused the sample set to vary from other sample sets in most comparable references. Elastic properties are generally calculated for homogeneous, isotropic materials in order to eliminate outside variables. Considering that this was not the case in this study, the results are more complex, but better reflect the actual materials encountered in practice.

The classification is still a work in progress because the study area did not encompass all lithologic variation in Kentucky. An effort was made to sample the greatest stratigraphic spread in the study area, but not all stratigraphic units could be sampled. This could skew perceptions of representative lithologies in the study area. For example, sandstones in the sample set were all massive and homogeneous although large numbers of crossbedded sandstones are known to occur in the study area. In addition, shale sampling is incomplete. Shales in Kentucky are often problematic in transportation construction; therefore, a more comprehensive shale sample set would be useful. In the future, sampling could be done selectively in order to assign strength and durability parameters to specific formations or poorly represented lithologies.

Density and Velocity

Density and velocity values had similar trends. Carbonate and siliciclastic values were distinctly different for these parameters, as was expected. Carbonates had higher density and velocity values than siliciclastics. Heterogeneous limestone consistently had the greatest variation, and this was also expected. Interbedded samples consistently tested as if they were carbonate samples, suggesting that siliciclastic components in the interbedded samples played a very minimal role in behavior. For compression and shear wave velocities, siliciclastic values increased with increasing grain size. Black shale sample results were consistently lower than for all other rock types. Future work could include using triaxial load chambers while making sonic velocity measurements in order to better mimic in situ stresses.

Coefficient of determination (R^2) values for density/velocity plots were expected to be high, indicating a linear trend, but this was not the case for the majority of lithologies. Siltstone and gray shale had low R^2 values (not exceeding 0.3 for shear or compression wave velocity/density analyses). This can be attributed to the heterogeneity of many of the samples, as well as differing mineralogical components and sample porosity. Conversely, some R^2 values of samples were high. Fine-grained limestone, nodular limestone, and sandstone had high R^2 values when density/compression wave velocity trends were analyzed. The same lithologies, as well as black shale, had high R^2 values for density/shear wave velocity trends. The high R^2 for fine-grained limestone and sandstone can be explained by the homogeneity of those samples; however, the high values for nodular limestone are difficult to understand.

Elastic Constants

Poisson's ratio values are good evidence of the effect of heterogeneity on sample behavior because negative values indicate anisotropy. The siliciclastic sample sets had more negative values than the carbonate sample sets. Siliciclastic samples are visually homogeneous, unlike many of the carbonate samples and the interbedded samples. The heterogeneous limestone Poisson's ratio values vary less than values for other elastic constants and also density and velocity values.

Shear modulus and Young's modulus values behave similarly. As siliciclastic grain size increases, shear modulus and Young's modulus values increase. This mimics sonic velocity trends.

Limestone with thin shale streaks has a greater spread than heterogeneous limestone for both moduli, which may indicate the importance of bedding. Interbedded samples behaved like carbonates.

Index Properties

Because of the importance of bearing capacity, compressive testing is frequently conducted and could certainly help in the prediction of material behavior. Homogeneity appears to be the most important factor regarding compressive strength testing. The more homogeneous the sample, the greater its strength. This was true for both carbonate and siliciclastic rock types. This may influence strength parameters appearing to be higher than they actually are (black shale) or lower than they actually are (siltstone), which most likely is the result of rock fabric. Slake durability results were binary; they were either high (greater than 80 percent) or low (less than 45 percent). Fissile shale samples had consistently low values.

Characterization of fine-grained siliciclastic lithologies (shales) is extremely important in Kentucky. This study was focused on carbonate-rich units and likely underrepresented the diversity of shales in the state. An in-depth study of those rocks using similar methodology is warranted. Slake durability values would be more useful if a more comprehensive shale sample set was tested.

When comparing elastic moduli to compressive strength, some homogeneous classification groupings were clustered, which supported the classification groupings and indicated the potential to predict material behavior in some lithologies.

General Conclusions

The creation of an empirical, repeatable classification focusing on carbonate-bearing rocks enabled lithologic comparisons. After cores were assigned a lithologic classification, sonic velocity, unconfined compressive strength, and slake durability testing was done in an attempt predict material behavior for each classification group. Carbonates behaved sporadically, especially with regard to heterogeneous limestone; however, sonic velocity results, as well as results for the other index tests, indicated that siliciclastic and carbonate samples behaved differently and somewhat predictably. Homogenous samples behaved similarly and were therefore easier to predict. Heterogeneous samples were quite varied and were harder to

predict. Overall, it is now feasible to view a cored rock sample in the field, classify it, and based on that classification, have some idea about its density, velocity, elastic behavior, strength, and durability.

APPENDIX

Appendix Table 1. Raw sample data, including all elastic constants and the lithologic classification.

Sample	Vs (m/s)	Vp (m/s)	Vp/Vs	Density (g/cm^3)	Young's Modulus (Gpa)	Shear Modulus (GPa)	Poisson's Ratio	Classification
11-2-	2,326.86	4,809.42	2.067	2.67	38.94	14.45	0.35	Limestone with thin shale streaks
13-12	895.36	540.19	0.603	2.52	9.24	2.02	1.29	Limestone, heterogeneous
14-5	1,381.84	2,356.47	1.705	2.49	11.79	4.76	0.24	Shale, gray
16-19	2,363.61	5,318.45	2.250	2.66	40.91	14.86	0.38	Interbedded
1-7-	2,109.15	5,124.62	2.430	2.69	33.40	11.95	0.40	Limestone, nodular
18-2	1,370.34	2,334.56	1.704	2.53	11.77	4.76	0.24	Shale, gray
20-3	1,353.75	1,924.57	1.422	2.56	9.50	4.70	0.01	Limestone, heterogeneous
2-12-	2,652.77	6,138.40	2.314	2.69	52.37	18.90	0.39	Limestone, coarse-grained
25-2	2,718.80	5,822.88	2.142	2.67	53.72	19.74	0.36	Limestone, coarse-grained
26-3	1,827.49	3,465.44	1.896	2.64	23.02	8.81	0.31	Limestone, nodular
26-5-s	2,018.10	3,647.32	1.807	2.64	27.46	10.73	0.28	Interbedded
26-6 s	2,502.78	4,865.01	1.944	2.68	44.31	16.79	0.32	Interbedded
27-1	2,123.17	4,422.18	2.083	2.67	32.50	12.04	0.35	Limestone, nodular
27-2	1,504.95	4,392.46	2.919	2.66	17.26	6.02	0.43	Interbedded
3_16	1,260.62	1,794.27	1.423	2.53	8.13	4.02	0.01	Shale, gray
31-9	738.66	5,569.06	7.539	2.68	4.36	1.46	0.49	Limestone with thin shale streaks
31-9+s	2,561.63	5,229.18	2.041	2.66	46.89	17.47	0.34	Limestone with thin shale streaks
32-6+s	2,312.71	5,419.40	2.343	2.64	39.19	14.11	0.39	Limestone with thin shale streaks
33-10-s	2,144.84	4,761.55	2.220	2.66	33.58	12.23	0.37	Limestone, heterogeneous
34-1	1,657.37	3,603.01	2.174	2.64	19.77	7.24	0.37	Limestone, heterogeneous

Sample	Vs (m/s)	Vp (m/s)	Vp/Vs	Density (g/cm^3)	Young's Modulus (Gpa)	Shear Modulus (GPa)	Poisson's Ratio	Classification
34-10 s	1,912.45	3,489.23	1.824	2.63	24.74	9.62	0.29	Limestone, heterogeneous
34-5	1,603.15	3,122.44	1.948	2.63	17.84	6.75	0.32	Limestone, heterogeneous
36-3 s	2,628.79	6,044.87	2.299	2.69	51.45	18.59	0.38	Interbedded
37+1+s	2,188.63	4,262.32	1.947	2.66	33.61	12.72	0.32	Interbedded
37-4	1,722.69	2,609.02	1.515	2.59	17.15	7.70	0.11	Shale, gray
37-4+s	1,798.96	2,993.88	1.664	2.61	20.57	8.45	0.22	Limestone, nodular
38-3	2,227.76	3,190.14	1.432	2.66	27.05	13.21	0.02	Limestone with thin shale streaks
38-4	1,562.30	2,476.44	1.585	2.62	14.97	6.40	0.17	Limestone, nodular
40-4-s	2,364.33	5,852.27	2.475	2.69	42.19	15.04	0.40	Limestone, coarse-grained
40-5	1,585.59	2,906.25	1.833	2.58	16.68	6.47	0.29	Limestone, heterogeneous
40-5+s	1,717.46	3,102.60	1.807	2.52	19.04	7.44	0.28	Shale, gray
40-6	1,752.79	2,967.48	1.693	2.49	18.87	7.66	0.23	Shale, gray
41-5	1,842.10	3,337.29	1.812	2.64	22.91	8.94	0.28	Limestone, nodular
44-1	2,157.80	5,084.50	2.356	2.70	34.97	12.58	0.39	Interbedded
46-3	2,481.86	5,169.77	2.083	2.61	43.35	16.05	0.35	Limestone, heterogeneous
46-7+s	1,800.72	2,924.40	1.624	2.64	20.42	8.55	0.19	Shale, gray
48-2-s	1,053.55	1,171.26	1.112	2.31	–3.18	2.56	–1.62	Shale, black
48-3 s	868.47	1,345.64	1.549	2.35	4.06	1.78	0.14	Shale, black
49-1	3,310.25	5,248.87	1.586	2.59	66.42	28.39	0.17	Limestone with thin shale streaks
5_6	1,267.18	1,723.77	1.360	2.50	7.31	4.01	-0.09	Shale, gray
50-2	2,701.31	5,526.65	2.046	2.67	52.26	19.46	0.34	Limestone, heterogeneous
50-22-s	2,336.90	4,734.28	2.026	2.68	39.23	14.65	0.34	Limestone, heterogeneous
50-3	2,826.20	5,733.93	2.029	2.62	56.17	20.97	0.34	Limestone with thin shale streaks
51-3	2,239.13	4,906.86	2.191	2.66	36.53	13.35	0.37	Limestone with thin shale streaks
51-4	2,460.83	5,420.76	2.203	2.66	44.11	16.10	0.37	Limestone with thin shale streaks

Sample	Vs (m/s)	Vp (m/s)	Vp/Vs	Density (g/cm^3)	Young's Modulus (Gpa)	Shear Modulus (GPa)	Poisson's Ratio	Classification
51-5 s	2,101.94	4,645.84	2.210	2.64	32.00	11.67	0.37	Limestone with thin shale streaks
52-spt-1	1,931.52	3,319.47	1.719	2.57	23.82	9.57	0.24	Sandstone
53-1	1,287.50	1,783.31	1.385	2.57	8.15	4.27	–0.04	Limestone, heterogeneous
53-2-s	1,988.10	3,561.52	1.791	2.63	26.48	10.40	0.27	Interbedded
53-3	2,047.38	3,029.50	1.480	2.62	23.70	10.98	0.08	Interbedded
54-5-s	1,311.16	2,341.03	1.785	2.57	11.22	4.41	0.27	Shale, gray
55-11+s	2,062.81	3,771.75	1.828	2.57	28.14	10.93	0.29	Siltstone
55-8-s	2,129.49	4,043.44	1.899	2.65	31.41	12.01	0.31	Interbedded
56-12 s	2,082.39	4,261.81	2.047	2.62	30.55	11.37	0.34	Limestone, heterogeneous
56-4+s	2,102.11	4,603.28	2.190	2.65	32.01	11.70	0.37	Limestone, fine-grained
56-7	1,722.44	3,435.84	1.995	2.57	20.35	7.64	0.33	Limestone, heterogeneous
57-4-s	1,668.50	4,037.36	2.420	2.69	20.90	7.48	0.40	Limestone, heterogeneous
57-9	2,802.15	6,161.29	2.199	2.65	56.93	20.78	0.37	Limestone, heterogeneous
61-1 s	1,197.85	1,559.24	1.302	2.29	5.13	3.29	–0.22	Shale, black
62-1 s	1,956.07	3,047.00	1.558	2.56	22.54	9.80	0.15	Shale, sandy
62-2 s	2,055.17	2,969.32	1.445	2.59	22.73	10.93	0.04	Siltstone
62-3 s	2,282.49	3,477.27	1.523	2.49	29.13	12.99	0.12	Siltstone
62-5s	1,738.26	3,154.41	1.815	2.56	19.81	7.73	0.28	Shale, sandy
63-1 s	2,436.78	4,257.94	1.747	2.62	39.11	15.56	0.26	Limestone, heterogeneous
65-1 s	1,157.37	4,554.63	3.935	2.59	10.18	3.47	0.47	Limestone, coarse-grained
65-3 s	2,291.18	5,128.72	2.238	2.46	35.48	12.90	0.38	Limestone, heterogeneous
65-4 s	2,594.50	5,599.84	2.158	2.65	48.72	17.87	0.36	Limestone, coarse-grained
66-3 s	2,530.82	4,917.33	1.943	2.80	47.29	17.91	0.32	Limestone with thin shale streaks
66-4 s	2,313.58	4,224.41	1.826	2.54	34.99	13.60	0.29	Limestone, coarse-grained
66-8 s	2,673.26	6,206.43	2.322	2.70	53.45	19.28	0.39	Limestone, coarse-grained

Sample	Vs (m/s)	Vp (m/s)	Vp/Vs	Density (g/cm^3)	Young's Modulus (Gpa)	Shear Modulus (GPa)	Poisson's Ratio	Classification
67-1 s	2,047.58	3,057.25	1.493	2.45	22.46	10.27	0.09	Limestone, fine-grained
67-2s	2,003.62	3,282.46	1.638	2.51	24.21	10.06	0.20	Siltstone
68-1 s	2,006.46	3,881.04	1.934	2.60	27.55	10.45	0.32	Limestone, coarse-grained
68-3 s	2,421.54	4,640.98	1.917	2.64	40.58	15.45	0.31	Limestone, coarse-grained
69-1 s	2,582.88	5,455.10	2.112	2.59	46.79	17.26	0.36	Siltstone
69-2 s	1,925.72	3,621.10	1.880	2.32	22.47	8.62	0.30	Interbedded
69-4 s	2,250.59	3,993.39	1.774	2.57	32.94	13.00	0.27	Siltstone
69-6 s	2,186.68	3,593.68	1.643	2.74	31.56	13.08	0.21	Siltstone
71-1s	2,728.86	5,849.87	2.144	2.68	54.23	19.93	0.36	Limestone, coarse-grained
71-2 s	2,066.04	3,610.79	1.748	2.59	27.78	11.05	0.26	Siltstone
71-3s	2,189.96	3,781.32	1.727	2.65	31.69	12.70	0.25	Interbedded
72-2 s	2,205.35	3,977.02	1.803	2.57	31.90	12.48	0.28	Siltstone
72-3s	1,777.38	3,650.52	2.054	2.51	21.35	7.94	0.34	Siltstone
74-4s	1,068.11	559.91	0.524	2.32	11.61	2.65	1.19	Shale, black
75-1s	1,262.48	1,691.48	1.340	2.57	7.15	4.10	–0.13	Shale, gray
75-3 s	2,349.50	4,031.87	1.716	2.42	33.22	13.37	0.24	Limestone, heterogeneous
75-4 s	1,908.58	3,278.87	1.718	2.53	22.94	9.22	0.24	Siltstone
75-5 s	1,805.90	2,564.80	1.420	2.47	16.26	8.06	0.01	Siltstone
76-1 s	1,928.70	5,804.20	3.009	2.89	30.92	10.75	0.44	Limestone, coarse-grained
76-2 s	2,692.40	6,451.96	2.396	2.69	54.45	19.52	0.39	Limestone, fine-grained
76-5 s	2,775.72	5,696.28	2.052	2.70	55.95	20.81	0.34	Limestone, fine-grained
77-1 s	2,682.78	5,418.41	2.020	2.66	51.12	19.11	0.34	Limestone, coarse-grained
77-2 s	2,667.11	5,828.21	2.185	2.66	51.84	18.95	0.37	Limestone, coarse-grained
78-1 s	2,479.20	5,618.77	2.266	2.75	46.69	16.93	0.38	Limestone, coarse-grained
79-4 s	2,941.37	5,565.71	1.892	2.64	59.56	22.80	0.31	Limestone, coarse-grained

Sample	Vs (m/s)	Vp (m/s)	Vp/Vs	Density (g/cm^3)	Young's Modulus (Gpa)	Shear Modulus (GPa)	Poisson's Ratio	Classification
79-5 s	2,219.14	4,039.60	1.820	2.33	29.46	11.47	0.28	Dolostone
79-6 s	2,094.47	3,658.31	1.747	2.58	28.47	11.33	0.26	Interbedded
79-7 s	1,367.42	1,826.03	1.335	2.59	8.36	4.85	–0.14	Siltstone
80-2s	1,672.23	2,635.94	1.576	2.47	16.06	6.91	0.16	Shale, gray
80-3 s	1,502.78	2,207.69	1.469	2.47	11.90	5.57	0.07	Limestone with thin shale streaks
80-5 s	1,093.18	1,266.41	1.158	2.53	0.23	3.03	–0.96	Shale, gray
82-1s	1,178.19	1,565.89	1.329	2.49	5.86	3.46	–0.15	Shale, gray
82-3 s	1,464.30	2,212.03	1.511	2.29	10.89	4.91	0.11	Sandstone
82-4 s	2,506.19	5,240.74	2.091	2.72	46.24	17.10	0.35	Sandstone
82-5 s	1,521.13	2,136.76	1.405	2.34	10.66	5.40	–0.01	Siltstone
83-1 s	2,395.58	5,973.35	2.493	2.62	42.16	15.01	0.40	Limestone, coarse-grained
83-2s	1,295.80	1,561.40	1.205	2.62	3.46	4.39	–0.61	Limestone, fine-grained
83-4 s	2,655.07	5,940.63	2.237	2.67	51.75	18.82	0.38	Limestone, coarse-grained
84-3s	1,918.51	4,220.10	2.200	2.69	27.16	9.91	0.37	Limestone, heterogeneous
85-3 s	2,425.18	5,551.42	2.289	2.69	43.74	15.83	0.38	Limestone, fine-grained
85-5 s	2,247.57	4,444.24	1.977	2.49	33.37	12.56	0.33	Limestone, heterogeneous
85-6 s	2,727.68	5,272.36	1.933	2.69	52.74	20.02	0.32	Limestone, fine-grained
85-7 s	2,277.54	5,909.41	2.595	2.67	39.19	13.87	0.41	Limestone, coarse-grained
85-8 s	2,432.05	5,212.13	2.143	2.67	43.06	15.82	0.36	Limestone, coarse-grained

Appendix Table 2. Compression strength and slake durability values.

Sample	Classification	Compression (psi)	Slake Durability Index (%)
20-3	Limestone, heterogeneous	3,260	
2-12-	Limestone, coarse-grained	15,790	
25-2	Limestone, coarse-grained	12,500	
26-3	Limestone, nodular	5,850	
27-2	Interbedded		96.9
3_16	Shale, gray	8,560	
31-9+s	Limestone with thin shale streaks	9,310	
34-10 s	Limestone, heterogeneous	7,580	
34-5	Limestone, heterogeneous	5,570	
36-3 s	Interbedded	18,660	
37-4	Shale, gray		89.4
37-4+s	Limestone, nodular	9,450	
38-3	Limestone with thin shale streaks	3,410	
38-4	Limestone, nodular		89.5
40-6	Shale, gray		95.3
44-1	Interbedded	7,680	
46-7+s	Shale, gray		89.1
48-2-s	Shale, black	15,240	97.5
48-3 s	Shale, black		98.1
5_6	Shale, gray		89.5
50-2	Limestone, heterogeneous	11,180	
51-3	Limestone with thin shale streaks	6,580	
51-5 s	Limestone with thin shale streaks	6,250	
53-1	Limestone, heterogeneous		82.4
53-2-s	Interbedded	7,320	

Sample	Classification	Compression (psi)	Slake Durability Index (%)
56-12 s	Limestone, heterogeneous	11,230	
57-9	Limestone, heterogeneous	11,270	
61-1 s	Shale, black	13,610	97.9
62-1 s	Shale, sandy		95.6
62-5s	Shale, sandy		96.2
66-8 s	Limestone, coarse-grained	11,390	
74-4s	Shale, black		95.6
75-1s	Shale, gray		31.7
76-5 s	Limestone, fine-grained	16,160	
77-1 s	Limestone, coarse-grained	11,760	
77-2 s	Limestone, coarse-grained	15,460	
79-4 s	Limestone, coarse-grained	12,940	
79-5 s	Dolostone	7,700	
80-2s	Shale, gray	11,420	95.8
80-3 s	Limestone with thin shale streaks		95.2
82-5 s	Siltstone	7,610	
83-4 s	Limestone, coarse-grained	10,020	

Appendix Table 3. Sample location and stratigraphic information.

Sample	Classification	Depth (ft.)	County	Stratigraphic Estimate
11-2-	Limestone with thin shale streaks	6.5	Kenton	Fairview Fm./Kope Fm.
13-12	Limestone, heterogeneous	7	Gallatin	Bull Fork Fm./Grant Lake Fm./Fairview Fm./Kope Fm.
14-5	Shale, gray	9	Kenton	Grant Lake Fm./Fairview Fm.
16-19	Interbedded	27	Gallatin	Bull Fork Fm./Grant Lake Fm./Fairview Fm./Kope Fm.
1-7-	Limestone, nodular	26.5	Robertson	Tanglewood Limestone Mbr./Clays Ferry Fm.
18-2	Shale, gray	86.5	Campbell	Kope Fm.
20-3	Limestone, heterogeneous	25.5	Kenton	Bull Fork Fm.
2-12-	Limestone, coarse-grained	26.8	Robertson	Tanglewood Limestone Mbr./Millersburg Mbr.
25-2	Limestone, coarse-grained	20.3	Harrison	Clays Ferry Fm./Tanglewood Limestone Mbr.
26-3	Limestone, nodular	47.3	Garrard	Lower Lexington Limestone/Tanglewood Limestone Mbr.
26-5-s	Interbedded	55.7	Garrard	Lower Lexington Limestone/Tanglewood Limestone Mbr.
26-6 s	Interbedded	64	Garrard	Lower Lexington Limestone/Tanglewood Limestone Mbr.
27-1	Limestone, nodular	12.5	Garrard	Ashlock Fm./Calloway Creek Limestone
27-2	Interbedded	13.5	Garrard	Ashlock Fm./Calloway Creek Limestone
3_16	Shale, gray	67.75	Campbell	Kope Fm.
31-9	Limestone with thin shale streaks	62.5	Pendleton	Clays Ferry Fm.
31-9+s	Limestone with thin shale streaks	62.5	Pendleton	Clays Ferry Fm.
32-6+s	Limestone with thin shale streaks	24.5	Scott	Tanglewood Limestone Mbr.
33-10-s	Limestone, heterogeneous	41.7	Harrison	Clays Ferry Fm./Tanglewood Limestone Mbr.

Sample	Classification	Depth (ft.)	County	Stratigraphic Estimate
34-1	Limestone, heterogeneous	8	Clark	Upper part of the Lexington Limestone
34-10 s	Limestone, heterogeneous	34	Clark	Upper part of the Lexington Limestone
34-5	Limestone, heterogeneous	24	Clark	Upper part of the Lexington Limestone
36-3 s	Interbedded	21.7	Montgomery	Calloway Creek Limestone
37+1+s	Interbedded	10.2	Montgomery	Calloway Creek Limestone
37-4	Shale, gray	28.8	Montgomery	Calloway Creek Limestone
37-4+s	Limestone, nodular	28.4	Montgomery	Calloway Creek Limestone
38-3	Limestone with thin shale streaks	20	Montgomery	Calloway Creek Limestone
38-4	Limestone, nodular	21.9	Montgomery	Calloway Creek Limestone
40-4-s	Limestone, coarse-grained	6	Grant	Fairview Fm.
40-5	Limestone, heterogeneous	7	Grant	Fairview Fm.
40-5+s	Shale, gray	7	Grant	Fairview Fm.
40-6	Shale, gray	9	Grant	Fairview Fm.
41-5	Limestone, nodular	33.4	Harrison	Clays Ferry Fm./Tanglewood Limestone Mbr.
44-1	Interbedded	12	Scott	Clays Ferry Fm.
46-3	Limestone, heterogeneous	13.2	Oldham	Laurel Dolomite
46-7+s	Shale, gray	33	Oldham	Laurel Dolomite
48-2-s	Shale, black	10.8	Jefferson	New Albany Shale
48-3 s	Shale, black	15.5	Jefferson	New Albany Shale
49-1	Limestone with thin shale streaks	9.6	Jessamine	Lower Lexington Limestone
5_6	Shale, gray	32.3	Robertson	Tanglewood Limestone Mbr., Grier Limestone Mbr.
50-2	Limestone, heterogeneous	16	Jefferson	Undetermined
50-22-s	Limestone, heterogeneous	151.3	Jefferson	Undetermined
50-3	Limestone with thin shale	31.7	Jefferson	Undetermined

Sample	Classification	Depth (ft.)	County	Stratigraphic Estimate
	streaks			
51-3	Limestone with thin shale streaks	13.2	Franklin	Lower Lexington Limestone
51-4	Limestone with thin shale streaks	14	Franklin	Lower Lexington Limestone
51-5 s	Limestone with thin shale streaks	14.33	Franklin	Lower Lexington Limestone
52-spt-1	Sandstone	3.9	Oldham	Drakes Formation
53-1	Limestone, heterogeneous	8.3	Shelby	Grant Lake Fm./Calloway Creek Limestone
53-2-s	Interbedded	9.7	Shelby	Grant Lake Fm./Calloway Creek Limestone
53-3	Interbedded	19	Shelby	Grant Lake Fm./Calloway Creek Limestone
54-5-s	Shale, gray	44	Henry	Bull Fork Fm.
55-11+s	Siltstone	117.6	Jefferson	Undetermined
55-8-s	Interbedded	93.3	Jefferson	Undetermined
56-12 s	Limestone, heterogeneous	114.2	Henry/Owen	Grier Limestone Mbr./Tanglewood Limestone Mbr.
56-4+s	Limestone, fine-grained	91.4	Henry/Owen	Grier Limestone Mbr./Tanglewood Limestone Mbr.
56-7	Limestone, heterogeneous	103.6	Henry/Owen	Grier Limestone Mbr./Tanglewood Limestone Mbr.
57-4-s	Limestone, heterogeneous	19.35	Franklin	Lower Lexington Limestone
57-9	Limestone, heterogeneous	26.8	Franklin	Lower Lexington Limestone
61-1 s	Shale, black	17.4	Casey	New Albany Shale
62-1 s	Shale, sandy	29.3	Casey	Undetermined
62-2 s	Siltstone	47	Casey	Undetermined
62-3 s	Siltstone	77.5	Casey	Undetermined
62-5s	Shale, sandy	143	Casey	Undetermined
63-1 s	Limestone, heterogeneous	5	Adair	Fort Payne Fm.

Sample	Classification	Depth (ft.)	County	Stratigraphic Estimate
65-1 s	Limestone, coarse-grained	6.7	Adair	Fort Payne Fm., Reef limestone
65-3 s	Limestone, heterogeneous	29.5	Adair	Fort Payne Fm., Reef limestone
65-4 s	Limestone, coarse-grained	35	Adair	Fort Payne Fm., Reef limestone
66-3 s	Limestone with thin shale streaks	36.6	Adair	Fort Payne Fm.
66-4 s	Limestone, coarse-grained	41.1	Adair	Fort Payne Fm.
66-8 s	Limestone, coarse-grained	49	Adair	Fort Payne Fm.
67-1 s	Limestone, fine-grained	18.2	Lincoln/Rockcastle	Undetermined
67-2s	Siltstone	27.8	Lincoln/Rockcastle	Undetermined
68-1 s	Limestone, coarse-grained	8.2	Adair	Fort Payne Fm.
68-3 s	Limestone, coarse-grained	53.7	Adair	Fort Payne Fm.
69-1 s	Siltstone	8.6	Data not provided	Undetermined
69-2 s	Interbedded	10.6	Data not provided	Undetermined
69-4 s	Siltstone	20	Data not provided	Undetermined
69-6 s	Siltstone	25.9	Data not provided	Undetermined
71-1s	Limestone, coarse-grained	23.1	Clinton	Salem and Warsaw Fm.
71-2 s	Siltstone	55.7	Clinton	Salem and Warsaw Fm.
71-3s	Interbedded	62.4	Clinton	Salem and Warsaw Fm.
72-2 s	Siltstone	20.3	Clinton	Salem and Warsaw Fm.
72-3s	Siltstone	24.5	Clinton	Salem and Warsaw Fm.
74-4s	Shale, black	40.7	Lincoln/Rockcastle	New Albany Shale
75-1s	Shale, gray	30.5	Rockcastle	Renfro Mbr.
75-3 s	Limestone, heterogeneous	36.4	Rockcastle	Renfro Mbr.
75-4 s	Siltstone	43.1	Rockcastle	Renfro Mbr.
75-5 s	Siltstone	50.8	Rockcastle	Renfro Mbr.
76-1 s	Limestone, coarse-grained	2.2	Pulaski	Kidder Limestone Mbr./Ste. Genevieve Limestone Mbr.

Sample	Classification	Depth (ft.)	County	Stratigraphic Estimate
76-2 s	Limestone, fine-grained	6.9	Pulaski	Kidder Limestone Mbr./Ste. Genevieve Limestone Mbr.
76-5 s	Limestone, fine-grained	42.9	Pulaski	Kidder Limestone Mbr./Ste. Genevieve Limestone Mbr.
77-1 s	Limestone, coarse-grained	10	Rockcastle	Ste. Genevieve Limestone Mbr.
77-2 s	Limestone, coarse-grained	17.3	Rockcastle	Ste. Genevieve Limestone Mbr.
78-1 s	Limestone, coarse-grained	3.5	Pulaski	Kidder Limestone Mbr.
79-4 s	Limestone, coarse-grained	29.2	Pulaski	St. Louis Limestone Mbr./Salem and Warsaw
79-5 s	Dolostone	40	Pulaski	St. Louis Limestone Mbr./Salem and Warsaw
79-6 s	Interbedded	49	Pulaski	St. Louis Limestone Mbr./Salem and Warsaw
79-7 s	Siltstone	49.5	Pulaski	St. Louis Limestone Mbr./Salem and Warsaw
80-2s	Shale, gray	22.3	Rockcastle	Borden/Renfro Mbr.
80-3 s	Limestone with thin shale streaks	24	Rockcastle	Borden/Renfro Mbr.
80-5 s	Shale, gray	48	Rockcastle	Borden/Renfro Mbr.
82-1s	Shale, gray	11.5	Rockcastle	Halls Gap Member of the Borden
82-3 s	Sandstone	23.7	Rockcastle	Halls Gap Member of the Borden
82-4 s	Sandstone	30.9	Rockcastle	Halls Gap Member of the Borden
82-5 s	Siltstone	33.2	Rockcastle	Halls Gap Member of the Borden
83-1 s	Limestone, coarse-grained	8.3	Pulaski	Ste. Genevieve Limestone Mbr.
83-2s	Limestone, fine-grained	19.9	Pulaski	Ste. Genevieve Limestone Mbr.
83-4 s	Limestone, coarse-grained	52.4	Pulaski	Ste. Genevieve Limestone Mbr.
84-3s	Limestone, heterogeneous	28.9	Cumberland	Fort Payne Fm.
85-3 s	Limestone, fine-grained	64.8	Pulaski	Ste. Genevieve Limestone Mbr./St. Louis Limestone Mbr.
85-5 s	Limestone, heterogeneous	72.3	Pulaski	Ste. Genevieve Limestone Mbr./St. Louis Limestone Mbr.
85-6 s	Limestone, fine-grained	75.6	Pulaski	Ste. Genevieve Limestone Mbr./St. Louis

Sample	Classification	Depth (ft.)	County	Stratigraphic Estimate
				Limestone Mbr.
85-7 s	Limestone, coarse-grained	152.6	Pulaski	Ste. Genevieve Limestone Mbr./St. Louis Limestone Mbr.
85-8 s	Limestone, coarse-grained	176.6	Pulaski	Ste. Genevieve Limestone Mbr./St. Louis Limestone Mbr.

REFERENCES CITED

ASTM, 1984, Standard D 2845, Annual book of ASTM Standards 4.08, Philadelphia, Pa.

Barnhill, M.L., and Zhou, H., 1996, Corebook of Pennsylvanian rocks in the Illinois Basin: Indiana Geological Survey, Illinois Basin Consortium, 19 p.

Birch, F., 1960, The velocity of compressional waves in rocks to 10 kilobars: Part I: Journal of Geophysical Research, v. 65, p. 1083–1102.

Burger, H., 1992, Exploration geophysics of the shallow subsurface: Englewood Cliffs, N.J., Prentice-Hall, 489 p.

Cressman, E.R., 1973, Lithostratigraphy and depositional environments of the Lexington Limestone (Ordovician) of central Kentucky: U.S. Geological Survey Professional Paper 768, 61 p.

Cressman, E.R., and Noger, M.C., 1976, Tidal-flat carbonate environments in the High Bridge Group (Middle Ordovician) of central Kentucky: Kentucky Geological Survey, ser. 10, Report of Investigations 18, 15 p.

Deere, D., and Miller, R., 1966, Engineering classification and index properties for intact rock: University of Illinois Air Force Weapons Lab Technical Report AFWLTR-65-116, 327 p.

Dunham, R., 1962, Classification of carbonate rocks according to depositional texture: *in* Ham, W. E. (ed.), Classification of carbonate rocks: American Association of Petroleum Geologists Memoir, p. 108-121.

Farmer, I., 1983, Engineering behaviour of rocks: London, Chapman and Hall London. 208 p.

Ferm, J., and Smith, G., 1981, A guide to cored rocks in the Pittsburgh Basin: University of Kentucky Department of Geology, 109 p.

Ferm, J., and Weisenfluh, G., 1981, Cored rocks of the southern Appalachian coal fields: University of Kentucky Department of Geology, 93 p.

Ferm, J., Smith, G., Weisenfluh, G., and DuBois, S., 1985, Cored rocks in the Rocky Mountain and High Plains coal fields: University of Kentucky Department of Geology, 90 p.

Folk, R., 1959, Practical petrographic classification of limestones: American Association of Petroleum Geologists Bulletin, v. 43, no. 1, p. 1–38.

Gaviglio, P., 1989, Longitudinal waves propagation in a limestone: The relationship between velocity and density: Rock Mechanics and Rock Engineering, v. 22, no. 4, p. 299–306.

Gercek, H., 2007, Poisson's ratio values for rocks: International Journal of Rock Mechanics and Mining Sciences, v. 44, no. 1, p. 1–13.

Hack, R., and Huisman, M., 2002, Estimating the intact rock strength of a rock mass by simple means, *in* van Rooy, J.L., and Jermy, C.A., eds., Engineering geology for developing countries: Proceedings of the 9th Congress of the International Association for Engineering Geology and the Environment, Durban, South Africa, 16–20 September 2002, p. 1971–1977.

Johnston, J., and Christensen, N., 1993, Compressional to shear velocity ratios in sedimentary rocks: International Journal of Rock Mechanics and Mining Sciences, v. 30, p. 751–754.

Jones, L., and Wang, H., 1981, Ultrasonic velocities in Cretaceous shales from the Williston Basin: Geophysics, v. 46, p. 288.

Kentucky Transportation Cabinet, 2005, Geotechnical manual: Frankfort, Ky.

King, M., 1998, Petrophysics studies of sedimentary rocks from a cross-hole seismic test site: International Journal of Rock Mechanics and Mining Sciences, v. 35, no. 3, p. 279–289.

McDowell, R.C., 1986, The geology of Kentucky: A text to accompany the geologic map of Kentucky: U.S. Geological Survey Professional Paper 1151-H, 76 p.
Molina, G.M., and Mark, C., 1996, Rating the strength of coal mine roof rocks: U.S. Bureau of Mines Information Circular 9444, 20 p.
Peterson, W.L., 1981, Lithostratigraphy of the Silurian rocks exposed on the west side of the Cincinnati Arch in Kentucky: U.S. Geological Survey Professional Paper 1151-C, 29 p.
Pickett, G., 1963, Acoustic character logs and their applications in formation evaluation: Journal of Petroleum Technology, v. 15, no. 6, p. 659–667.
Sable, E.G., and Dever, G.R., Jr., 1990, Mississippian rocks in Kentucky: U.S. Geological Survey Professional Paper 1503, 125 p.
Smath, R.A., 1983, Discriminating relationships among basic lithologies and engineering parameters obtained from the point-load and slake durability tests: Richmond, Eastern Kentucky University, master's thesis, 173 p.
Tatham, R., 1982, Vp/Vs and lithology: Geophysics, v. 47, no. 3, p. 336–344.
Weir, G.W., Peterson, W.L., and Swadley, W C, 1984, Lithostratigraphy of Upper Ordovician strata exposed in Kentucky: U.S. Geological Survey Professional Paper 1151-E, 121 p.
West, T.R., 1994, Geology applied to engineering: Englewood Cliffs, N.J., Prentice Hall, 560 p.
Wilkens, R., Simmons, G., and Caruso, L., 1984, The ratio Vp/Vs as a discriminant of composition for siliceous limestones: Geophysics, v. 49, p. 1850.
Yasar, E., and Erdogan, Y., 2004, Correlating sound velocity with the density, compressive strength and Young's modulus of carbonate rocks: International Journal of Rock Mechanics and Mining Sciences, v. 41, p. 871.

Vita

BETHANY LEIGH OVERFIELD
D.O.B.: July 10, 1977
Henderson, Kentucky, USA

PRIOR EDUCATION

Western Kentucky University, Bowling Green, KY - Department of Geography and Geology
BS in Geology, Geography, August 2001

PRIOR EXPERIENCE

Kentucky Geological Survey - University of Kentucky, Lexington, KY
Geologist II Geologic Mapping Section, 08/01 – present

SELECTED PUBLICATIONS

Reports/Maps

Carey, D.I., Paylor, R.L., and **Overfield, B.L.,** 2006, Generalized geologic map for land-use planning: McCreary County, Kentucky, Kentucky Geological Survey Map and Chart Series 144-12, 1 p.

Carey, D.I., **Overfield, B.L.,** and Paylor, R.L., 2006, Generalized geologic map for land-use planning: Whitley County, Kentucky, Kentucky Geological Survey Map and Chart Series 141-12, 1 p.

Overfield, B.L., Weisenfluh, G.A., Andrews, W. A., 2004, Availability of Coal Resources for the Development of Coal: Davis (W. Ky. No. 6) and Dekoven (W. Ky. No. 7) Coals: Kentucky Geological Survey, Open File Report, 52 p.

Abstracts of Research Presented at Professional Meetings

Weisenfluh, G.A., **Overfield, B.L.,** Wang, R., 2010, Analysis of the geologic context of maintenance costs for rockfalls and landslides in Kentucky, [abs]: Geohazards in Transportation in Appalachia conference, Columbus, OH, August, 2010.

Overfield, B.L., Weisenfluh, G.A., Eble, C.F., 2005, Coal washability data trends in eastern Kentucky [abs]: Eastern Section meeting of the American Association of Petroleum Geologists, Morgantown, West Virginia, September, 2005.

Overfield, B.L., Andrews, W.M. Jr., Weisenfluh, G.A., 2002, Coal resource estimates—communicating results to the public: Geological Society of America Abstracts with Programs, Combined North-central-Southeastern section meeting, Lexington, Ky., v. 34.